

Metamorphic evolution of the Austroalpine units east of the Tauern Window: indications for Jurassic strike slip tectonics

by

Ralf SCHUSTER & Wolfgang FRANK

with 8 Figures, 3 Tables and 1 Plate

Keywords:

Austroalpine basement units
Jurassic tectonics
Metamorphism
Geochronology
Palaeogeography

Schlüsselwörter:

Austroalpin
Jurassische Tektonik
Metamorphose
Geochronologie
Paläogeographie

Addresses of the authors:

Dr. RALF SCHUSTER, Prof. Dr. WOLFGANG FRANK
Institut für Geologie, Universität Wien, UZA II
Althanstraße 14

A-1090 Wien

E-mail:

Dr. Ralf Schuster: Schuster.Ralf@univie.ac.at

Prof. Dr. Wolfgang Frank: Wolfgang.Frank@univie.ac.at

Contents

Kurzfassung, Abstract.....	38
1. Introduction.....	38
2. Regional settings.....	39
3. Analytical techniques.....	42
4. Investigated rock series and lithologies.....	44
4.1. The Wölz Crystalline Complex.....	44
4.1.1. Prograde assemblages in the Ramingstein Window.....	44
4.1.2. Polyphase assemblages from the eastern Wölz Complex.....	47
4.1.3. Metamorphic zonation of the Wölz Complex.....	48
4.2. The Bundschuh Complex.....	48
4.3. The Bundschuh thrust.....	50
5. Discussion.....	51
5.1. Comparison of sections through the Austroalpine basement units.....	51
5.2. The pre-Alpine paleogeographic position of the Bundschuh Complex.....	53
5.3. The sedimentary cover of the „Middle Austroalpine“.....	54
Acknowledgements.....	54
References.....	54

Kurzfassung

Durch petrologische und geochronologische Untersuchungen kann im Ostalpinen Kristallin östlich des Tauern Fensters eine duktile Überschiebungszone belegt werden, die den Bundschuh Komplex vom unterlagernden Wölz Komplex trennt. Der polymetamorphe Bundschuh Komplex, welcher den Untergrund der mesozoischen Stangalm Einheit bildet, wurde während der variszischen Orogenese amphibolitfaziell geprägt. Zur gleichen Zeit erlebte der heute unterlagernde Wölz Komplex maximal Bedingungen der unteren Grünschieferfazies. Diese Metamorphosezonierung impliziert einen tektonischen Kontakt der beiden Einheiten. Aufgrund lithologischer Übereinstimmungen zwischen dem Bundschuh Komplex und dem südlichen Teil des Ötztal Komplexes ist anzunehmen, daß der Bundschuh Komplex ebenso wie das Gurktaler Deckensystem bis in den Jura nahe dem südlichen Ötztal Komplex beheimatet war. Vermutlich im Jura wurden diese Einheiten an sinistralen Seitenverschiebungen ostwärts bewegt. Im Zuge der kompressiven Eoalpinen Tektonik, um ca. 100 Ma, wurden sie auf den Wölz Komplex WNW-gerichtet aufgeschoben. Die minimale Überschiebungswerte beträgt 35 km. Danach ist eine kontinuierliche Metamorphosezonierung von amphibolitfaziellen Bedingungen im Liegenden bis zu grünschieferfaziellen Bedingungen im Hangenden der kristallinen Einheiten zu beobachten. Die permo-mesozoischen Deckserien des Wölz Komplexes, Teile der Nördlichen Kalkalpen, müssen vor oder während der Bundschuhüberschiebung von ihrem Untergrund abgesichert worden sein.

Abstract

Based on metamorphic petrology and geochronological investigations a major Eoalpine ductile thrust zone separating the Bundschuh Complex from the underlying Wölz Complex is identified within the Austroalpine basement units east of the Tauern Window. The polymetamorphic Bundschuh Complex, forming the base of the Mesozoic Stangalm

Unit, experienced medium-grade Hercynian metamorphism. In contrast the tectonically lower Wölz Complex reached not more than lower greenschist facies conditions at this time. Because of this observed metamorphic zonation the contact between the Bundschuh Complex and the Wölz Complex is tectonic. Due to palaeogeographic considerations and due to lithological similarities with crystalline rocks of the Ötztal Complex, we conclude that the Bundschuh Complex, and the Gurktal Nappe were situated in a westerly position, close to the southern Ötztal Complex until Jurassic times. Most probably during Jurassic times, these units were displaced eastwards along sinistral strike-slip faults. Middle Cretaceous compressional tectonics (c. 100 Ma) emplaced the Bundschuh Complex and the Gurktal Nappe onto the Wölz Complex. The minimum transport distance in WNW-direction is about 35 km. After that a continuous Eoalpine metamorphic gradation from amphibolite facies at the base to lower greenschist facies conditions at the top of the welded units developed. The original cover series of the Wölz Complex, parts of the Northern Calcareous Alps, were stripped off before or during the emplacement of the Bundschuh Complex.

1. Introduction

“Altkristallin” is a classic term for the vast masses of Austroalpine crystalline basement units. It is considered to represent a continuous tectonic unit, dominated by Hercynian amphibolite-grade metamorphism and corresponding penetrative deformation, whereas Alpine structures are limited to distinct deformation zones. Among other arguments, such considerations were used to establish the concept of the “Middle Austroalpine” by TOLLMANN (1959, 1977). According to this concept main parts of the “Altkristallin” form the Middle Austroalpine basement unit which is covered by Mesozoic sediments with special facies characteristics. They were deposited north of the Upper Austroalpine including the Northern Calcareous Alps (Fig. 1A). During the Eoalpine compressional event the Northern

Calcareous Alps have been stripped of from their basement and thrust to the northwest overriding the Middle and Lower Austroalpine. Except negligible volumes the Upper Austroalpine basement disappeared from the surface. Remnants of this Middle Austroalpine sedimentary cover occur mostly at the northern margin of the basement. However east of the Tauern Window the Stangalm Mesozoic overlies the central part (Fig. 2 and 3). This isolated Permo-Mesozoic sequence holds a key position in understanding

ne metamorphic events, the well known Hercynian and an additional high-temperature/low-pressure metamorphic event during Permo-Triassic times (SCHUSTER et al. 1999a, b).

In this paper we deal with the metamorphic evolution of the crystalline units below the Stangalm Mesozoic Unit. Informations from the basement units in the Stangalm area give important constraints for the palaeogeography of the

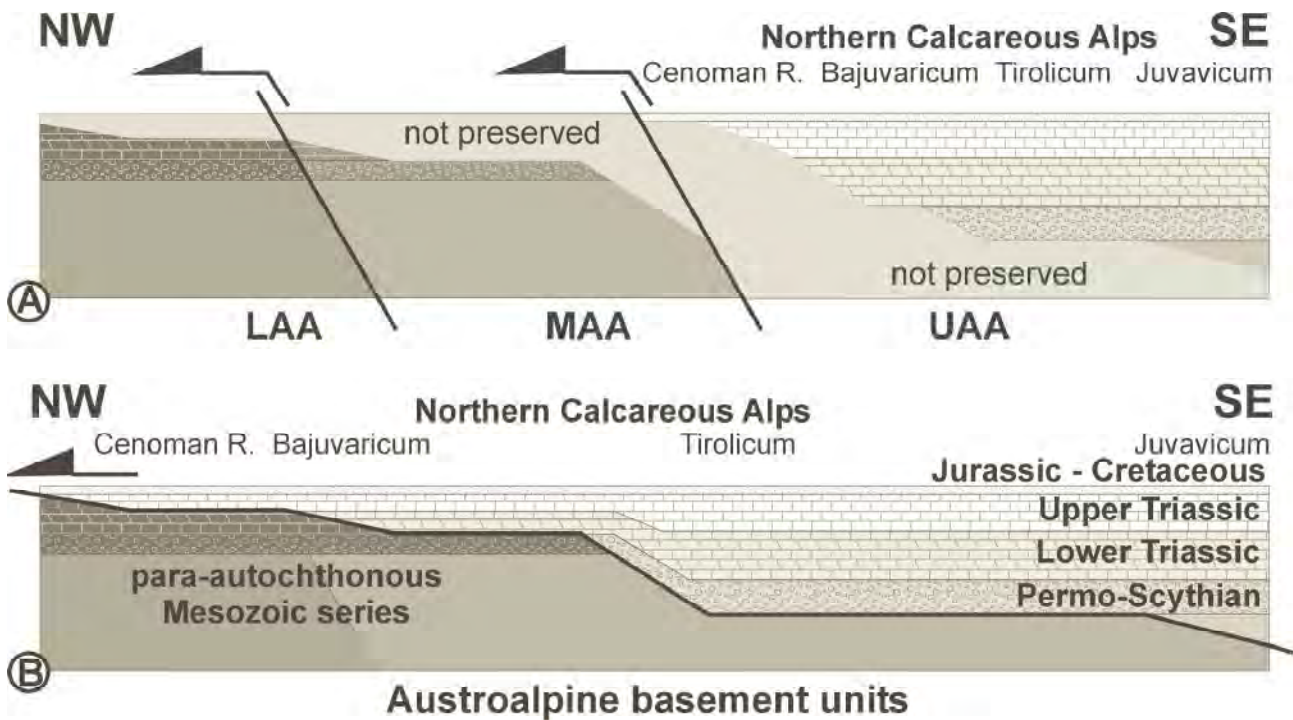


Fig. 1: Tectonostratigraphy of the Austroalpine units. (A) model according to TOLLMANN (1977). Per definition (e.g. TOLLMANN 1977, page 5) the Lower Austroalpine (LAA), Middle Austroalpine (MAA) and Upper Austroalpine (UAA) represent lateral neighbouring areas. (B) proposed model according to FRANK et al. (1983), GENSER & NEUBAUER (1989) and SCHUSTER et al. (1999a). In this model, LAA, MAA and UAA do not represent lateral neighbouring areas any more. Therefore, the nomenclature defined by TOLLMANN (1977) is not applicable using model B.

the evolution history of the Austroalpine tectonic realm. Various and contrasting models (among others: TOLLMANN 1965, CLAR 1965, TOLLMANN 1975, FRANK 1987) have been proposed to explain the present day arrangement of the lithotectonic units in the Stangalm area in respect of the mutually assumed Permo-Triassic palaeogeography.

Since the eighties it has been recognised, that the "Altkristallin" is not a Hercynian consolidated basement block. It rather consists of several nappe complexes that have been overprinted during the Eoalpine event to various degrees with an increasing metamorphic gradient from north to the south. In the northern Hercynian metamorphic units low temperature deformation in distinct zones was recognised e. g. in the Schladming Complex (SLAPANSKY & FRANK 1987) or in the Semmering and Wechsel Complexes (DALLMEYER et al. 1992). In contrast in the south an intense tectonic and metamorphic overprint reaching eclogite and amphibolite facies conditions has been noticed (MORAUF 1980, FRANK 1987, THÖNI & JAGOUTZ 1992, HOINKES et al. 1999). In the last years it was possible to distinguish two major pre-Alpi-

Austroalpine area during post-Hercynian, Jurassic and Eoalpine times and for the old problem to correlate Austroalpine Permo-Mesozoic cover series with their former basement.

2. Regional settings

According to TOLLMANN (1977) the tectonically deepest part of the Austroalpine in the investigated area, east of the Tauern Window, is the Lower Austroalpine (Fig. 3A) which comprises the frame of the Tauern Window and the Radstadt Nappe System. The Lower Austroalpine is tectonically covered by the Hercynian metamorphic Middle Austroalpine. Its lowest parts are the Schladming and Seckau Complexes in the north and the lithologically different Millstatt Complex in the south. These units are overlain by the vast mass of micaschists of the Wölz Complex, comprising the "Wölz Micaschists" in the area around Bretstein and Oberwölz, the "Aineck-Teuerlnock Serie" at the Katschberg pass and the Radenthein Complex. The uppermost crystalline units

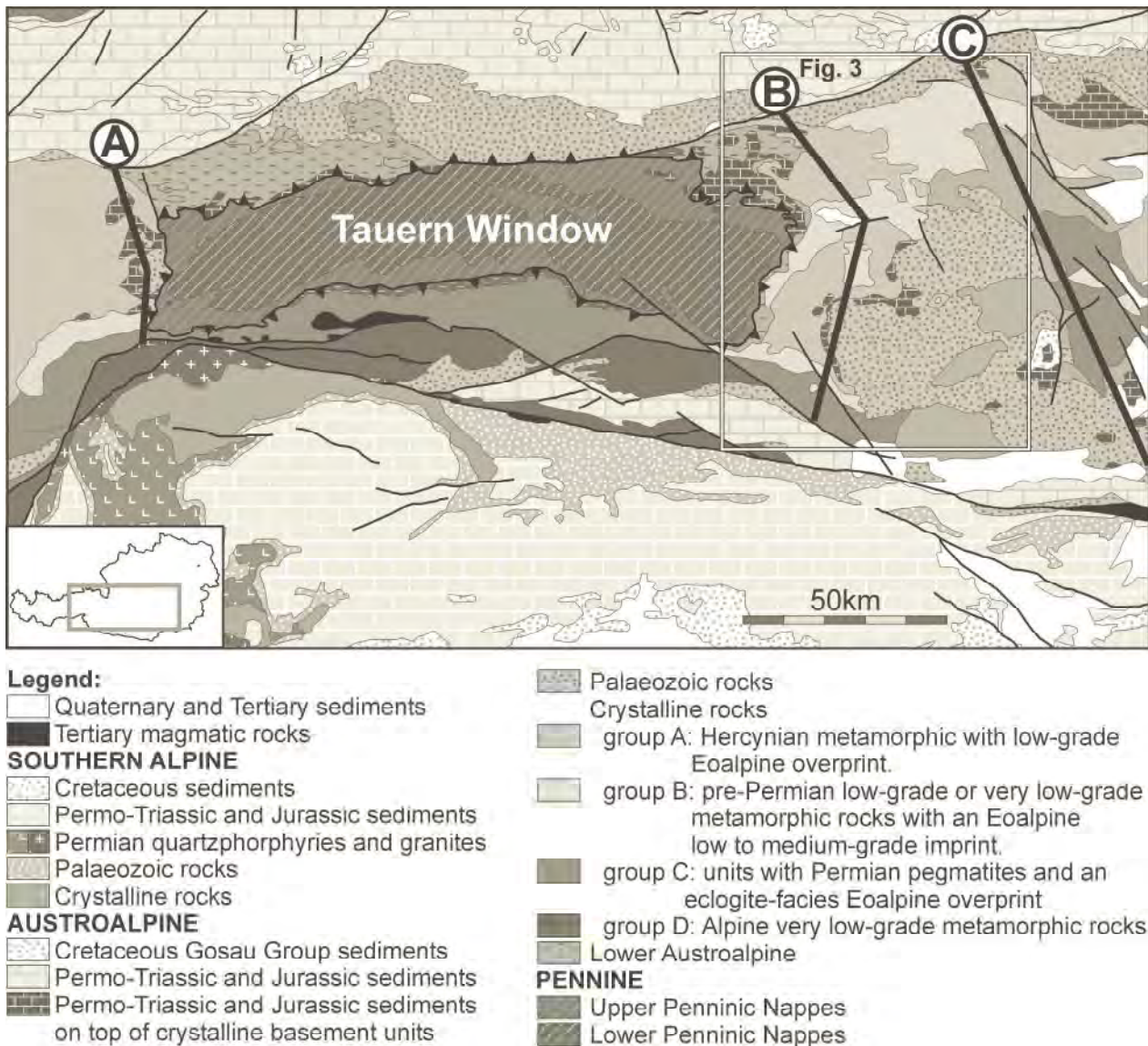


Fig. 2: Tectonic map of the Austroalpine. The subdivision of the crystalline units follows the discussion in SCHUSTER et al. (1999a). Lines A, B and C give the section lines of Fig. 7.

are the Bundschuh Complex in the west and the Saualm-Koralmbau Complex in the east. The para-autochthonous Mesozoic Stangalm Unit transgressed onto the Wölz Complex and the Bundschuh Complex. The tectonically highest unit is the Gurktal Nappe System, which is part of the Upper Austroalpine.

In recent years the Middle Austroalpine east of the Tauern Window has been mapped and investigated with modern geochronological and thermobarometrical methods by SLAPANSKY & FRANK (1987), FRIMMEL (1987, 1988), NOWAK

(1986), SCHIMANA (1986), THEINER (1987), BELOCKY (1988), SCHUSTER (1994), PISTOTNIK (1996) and KOROKNAI et al. (1999).

SCHIMANA (1986) discovered that the amphibolite facies assemblages in the micaschists of the Radenthein Complex are Eoalpine in age and derived from pre-Alpine garnet-free phyllites. In contrast, micaschists north of the Millstätter Alpe were recognised as polymetamorphic and part of the tectonically overlying polymetamorphic Bundschuh Complex (Fig. 3B). Thus a thrust contact between these units is deduced. Two major synmetamorphic Eoalpine and one

Fig. 3: Tectonic map of the Austroalpine east of the Tauern Window. Shown are the most important tectonic structures. (A) Model after TOLLMANN (1977): The Permo-Mesozoic Stangalm Unit transgresses onto the Hercynian welded Middle Austroalpine including the Schladming and Seckau Complexes, the "Lieser Paragneisses" (Bundschuh Complex and Millstatt Complex) and the Wölz Complex; (B) New interpretation compiled from SLAPANSKY & FRANK (1987), FRIMMEL (1987), SCHIMANA (1986), THEINER (1987) and SCHUSTER (1994). The crystalline basement units are subdivided in four groups by their metamorphic history according to SCHUSTER et al. (1999a). The Mesozoic Stangalm Unit transgresses only on top of the Bundschuh Complex. SAM = southern limit of Alpine Metamorphism (HOINKES et al. 1999).



- | | | |
|--|---|--------------------------------------|
| □ Quaternary and Tertiary sediments | ■ micaschists at the base of the Gurktal Nappe System | ■ S-KC Sau-Koralpe C. (S-KC) |
| AUSTROALPINE | ■ Drauzug Mesozoic | ■ WC Millstatt Complex (MC) group D: |
| Upper and "Middle" Austroalpine | ■ Goldeck phyllites | ■ GC Goldeck Complex (GC) |
| ■ Mesozoic and Palaeozoic rocks | Crystalline rocks | ■ GIC Gailtal Complex (GIC) |
| ■ Northern Calcareous Alps | group A: | Lower Austroalpine |
| ■ Greywackezone (Ennstal phyllites) | ■ SC Schladming C. (SC), | ■ Mesozoic sediments |
| ■ Gurktal Nappe System (GNS) | ■ BC Bundschuh C. (BC), | ■ metamorphic rocks |
| ■ Ackerl Nappe (crystalline rocks) | ■ ScC Seckau Complex (ScC) | PENNINE |
| ■ Stolzalpen Nappe | group B: | ■ Upper Penninic nappes |
| ■ Mesozoic sediments | ■ WC Wölz Complex (WC) | ■ Mesozoic sediments |
| ■ Carboniferous Stangnock Fm. | group C: | ■ basement rocks |
| ■ phyllitic rocks | ■ RC Rappolt Complex (RC) | ■ Lower Penninic nappes |
| ■ Murau Nappe | | |

major Tertiary deformation phase have been reported from this area: A first west- to northwest-directed simple shear deformation (D1) responsible for the development of the main schistosity (S1) is overprinted by north-south shortening (D2) forming a crenulation cleavage with steeply dipping axial planes (S2) (SCHIMANA 1986, BELOCKY 1988). The third deformation (D3) is an southeast-directed extensional event which affects the whole rock pile (GENSER & NEUBAUER 1989). D1 and D2 can be correlated with the two major superposed deformations during the Cretaceous collisional event. The third corresponds to the Tertiary extension of the Alpine orogene (RATSCHBACHER 1986, FROITZHEIM et al. 1996). THEINER (1987) described a similar structural and metamorphic evolution in the adjoining northwestern area near to the Katschberg Pass, but could not constrain the age of metamorphism of the "Aineck-Teuerlnockserie".

The eastern Wölz Complex (Bretstein and Sölk Pass area; Fig. 3B) was investigated by SCHIMANA (1984) and by ABART & MARTINELLI (1991). In the northeastern part they found only one garnet generation formed coevally with the steeply dipping Eoalpine axial planes of the crenulation cleavage (S2). In the east near Bretstein more than one garnet generation, with complex optical zonations, staurolite and Permian pegmatites (JÄGER & METZ 1971, SCHUSTER & THÖNI 1996) occur. The amphibolite facies assemblage formed

Complex and to address the relationship of the Wölz and Bundschuh Complexes by petrological studies and geochronological methods.

3. Analytical techniques

Minerals used for isotope determinations were hand-picked under a binocular microscope, except muscovite and biotite which were separated on a vibrating table and by grinding in alcohol. The potassium content of the mineral separates used for K-Ar measurements were determined by AAS-analyses on a PERKIN-ELMER 300 instrument.

For K-Ar dating about 30 mg of sample material was filled in cylindrical Ta-capsules and put in the Ar extraction line. Heating of the minerals was done by a RF-induction coil. Cleaning of the gas was performed by cold traps and Ti-sponge getters. Ar isotopic values were measured in a VG-5400 Fission Isotopes^R mass spectrometer. The ³⁸Ar spike volume was calibrated with laboratory standards and the international standard glauconite GL-O (24.69 ⁴⁰Ar_{rad} 10⁻⁶ cm³ STP g⁻¹). The errors given on the calculated age include only the 1σ error of the analytical data.

To remove surface contaminations mineral concentrates used for Sm-Nd and Rb-Sr analyses were leached in 2.5 N

Sample	Lithology	Unit	Locality	N	E
RSP20	paragneiss	BC	P, western slope of Karlsbergeck, alt. 1280 m	47°03'29"	013°55'41"
RSP35	paragneiss	BC	P, western slope of Karlsbergeck, alt. 1500 m	47°03'32"	013°56'01"
RSP44	graphitic micaschist	WC	P, Turrach road, west of Trattnerberg, alt. 1120 m	47°01'12"	013°54'05"
RSP53	garnet micaschist	WC	P, 400 m southwest of Goderitzberg, alt. 1360 m	47°05'07"	013°53'31"
RSP68	paragonite amphibolite	WC	P, 450 m east of Goderitzberg, alt. 1340 m	47°05'00"	013°54'20"
RSP69	quartzitic micaschist	WC	P, 500 m west of Goderitzberg, alt. 1360 m	47°05'02"	013°54'33"
RSP81	garnet micaschist	WC	P, 700 m west of Kendlbruck, alt. 1040 m	47°04'00"	013°52'08"
RSP86	amphibolite	WC	P, 1 km south of Altes Forsthaus, alt. 1190 m	46°59'02"	013°54'09"
RSP95	paragneiss	BC	P, 700 m northwest of Stieberhöhe, alt. 1700 m	47°02'49"	013°56'16"
RSP113	paragneiss	WC	P, 900 m north of Hannebauer, alt. 1360 m	47°00'08"	013°54'32"
RSP114	garnet micaschist	WC	P, 1.1km northeast of Hannebauer, alt. 1420 m	47°00'11"	013°54'52"
RSP119	paragneiss	BC	P, 1 km south of Tschaundinock, alt. 1690 m	47°00'31"	013°55'42"
RSP127	hornblende-paragneiss	BC	P, 900 m northwest of Strannerhöhe, alt. 1760 m	47°02'00"	013°56'26"
RSP131	paragneiss	BC	P, 350 m northwest of Stieberhöhe, 1770 m	47°02'35"	013°56'20"
RSP294	graphitic micaschist	WC	P, 1 km east of Grabenwirt, alt. 1500 m	47°03'20"	013°55'12"
RSP320	quartzitic gneiss	WC	P, 1.9 km east of Stierbrandhöhe, alt. 1490 m	47°01'21"	013°53'20"
RS6/95	garnet micaschist	WC	B, 1 km west of Bruderkogel, alt. 2045 m	47°23'27"	014°24'14"
RS44/97	garnet micaschist	WC	S, 500 m southwest of Glattjoch, alt. 1850 m	47°19'12"	014°13'11"

P...Predlitz east of Ramingstein, B...Bretstein valley, S...Schöttel valley north of Oberwölz

Tab. 1: GPS-coordinates and localities of the samples.

contemporaneously with a west to northwest-directed main structural imprint of the rocks and was assumed to be Hercynian in age. However the Permian pegmatites were affected by this deformation and therefore SCHIMANA (1984) also discussed an Eoalpine age of this event.

The aim of this study was to determine the age of the single and polyphase metamorphic assemblages of the Wölz

HCl before decomposition for 5 minutes at about 50 °C. Chemical sample digestion and element separation closely follows the procedure as described in THÖNI & JAGOUTZ (1992). Overall blank contributions are <0.2 ng for Nd, <0.1 ng for Sm, whereas <2 ng was determined for Sr and Rb. Sm and Nd concentrations were determined from separate mass spectrometer. Sr and Rb concentrations were measured

aliquots of the solution using a mixed REE (^{147}Sm - ^{150}Nd) spike. Contents of Rb and Sr were measured by isotope dilution, using a ^{87}Rb - ^{84}Sr spike. All Nd and Sm mineral

isotope ratios, as well as Sm and Nd spiked aliquots for concentration determinations, were run as metal ions from a Re double filament on a Finnigan[®] MAT262 multicollector

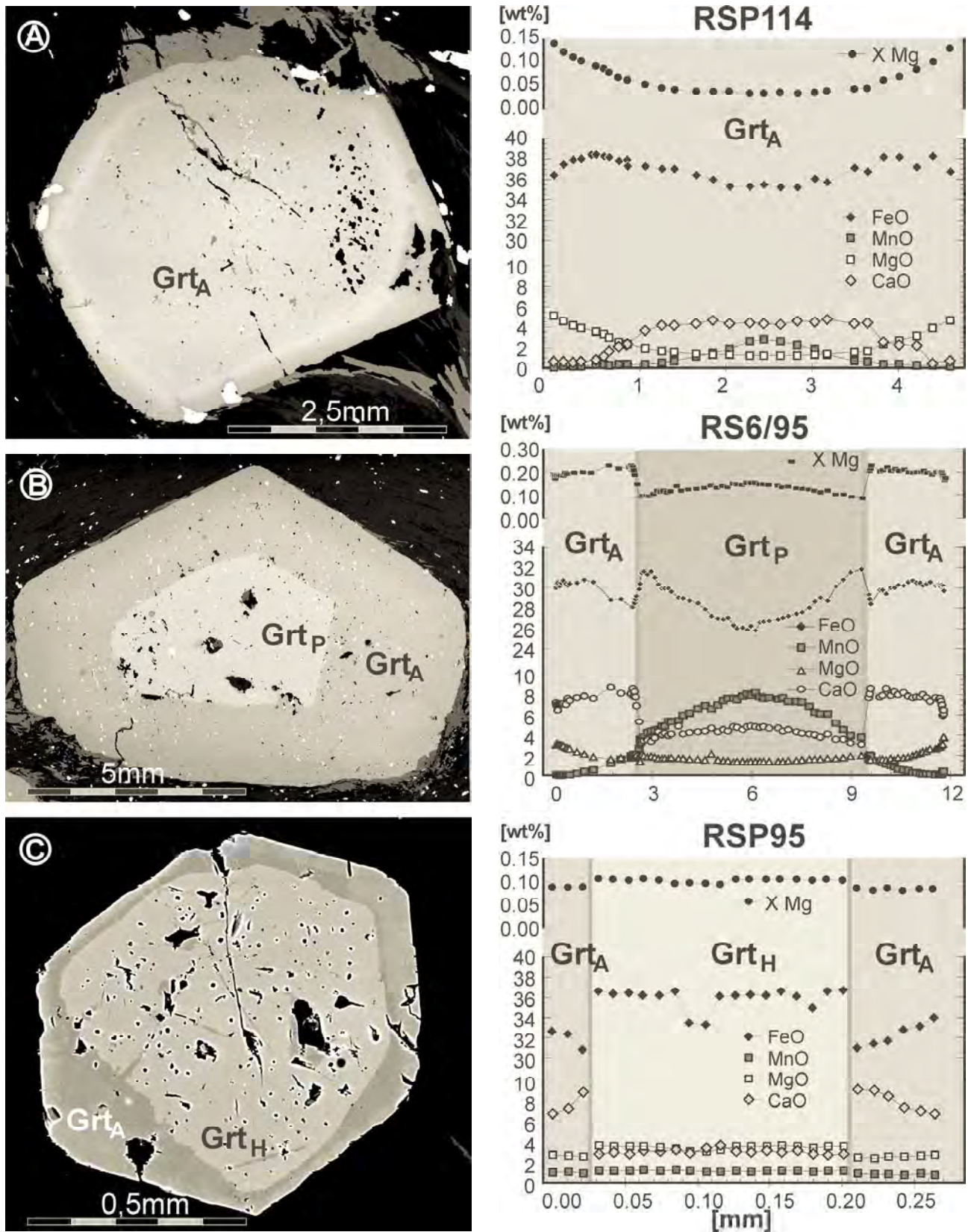


Fig. 4: BSE-images and chemical zonation pattern of representative garnets from the Wölz- and Bundschuh Complex (explanation see text): (A) Wölz Complex, Ramingstein Window (sample RSP114); (B) Wölz Complex, Bretstein valley (sample RS6/95); (C) Bundschuh Complex, frame of the Ramingstein Window (sample RSP95).

as metal species from a Ta single filament on a VG^R Micromass M30. During the relevant time interval the ¹⁴³Nd/¹⁴⁴Nd ratio for the La Jolla international standard was 0.511846±0.000008 whereas the value for the NBS 987 Sr standard was 0.71011±0.00006. Errors represent 2σ-mean deviations on block means. Maximum errors for ¹⁴⁷Sm/¹⁴⁴Nd and ⁸⁷Rb/⁸⁶Sr ratio are estimated to be ±1 %, based on spike re-calibration and iterative sample analysis.

Mineral composition data were obtained with an ARL SEMQ microprobe by energy and/or wavelength-dispersive spectrometry at the universities of Vienna and Innsbruck. Accelerating voltage was 15 kV and sample current 20 nA. Natural and synthetic standards were used for calibration.

4. Investigated rock series and lithologies

In the Ramingstein Window (Fig. 3B) the Wölz Complex is exposed in an asymmetrical anticline below the Bundschuh Complex. As there are several new road cuts with fresh outcrops this area was well suited to study the single phase assemblages of the Wölz Complex and their relationship to the polymetamorphic Bundschuh Complex. Polyphase micaschists of the Wölz Complex were sampled in the Bretstein valley, and in the Schöttel valley north of Oberwölz. GPS-coordinates of the sample localities are given in Tab. 1.

4.1. The Wölz Crystalline Complex

4.1.1. Prograde assemblages in the Ramingstein Window

The Wölz Complex in the Ramingstein Window consists of micaschists and graphitic micaschists with intercalations of quartzites, graphiteschists, amphibolites, paragonite-amphibolites and marbles. Detailed descriptions of the lithologies are given in SCHUSTER (1994), representative chemical analyses of the minerals are shown in Tab. 2. The micaschists and graphitic micaschists are characterised by the peak metamorphic assemblage Grt + St + Ky + Ms + Pl + Qtz + Rt. The main schistosity (S1) of the rocks is overprinted by a crenulation cleavage with east-west orientated axes and steeply dipping axial planes (S2).

Garnet crystals are normally 0.5 to 1cm in size (locally up to 7cm in diameter) and of idiomorphic shape in quartz-poor, mica-rich layers. They contain inclusions of quartz, ilmenite, rutile and rarely chloritoid and clinozoisite. Ilmenite inclusions occur in the central part of the garnet, whereas rutile is present near to the rim. The inclusion trails are still in contact with the external schistosity and argue for syn- to post deformative growth of the garnet during the formation of the schistosity S1 in a west- to northwest-directed simple shear or in a plain strain regime (Plate Fig. A, B). In the graphitic micaschists garnet often contains an inclusion-free core surrounded by graphite accumulations within cleavage domes.

The chemistry of the garnets is displayed as a representative profile in Fig. 4A. In general there is a continuous zonation in the garnet composition from core to rim with slight levelling up and then a reversal in the FeO content near to the rim. Pattern of increasing FeO, MgO and X_{MgO}-ratio and decreasing MnO and CaO are very common in medium-grade metapelites and usually indicative of growth during increasing temperature (LOOMIS & NIMICK 1982).

Chloritoid occurs very rarely as idiomorphic inclusions within the garnet (Plate Fig. B). The crystals are up to 2mm in size and show a homogeneous chemical composition. If they are not completely isolated from the matrix they are replaced by staurolite or muscovite and chlorite. Kyanite occurs as small crystals together with plagioclase around the garnet, especially in highly strained areas close to the crystal edges or between garnet porphyroblasts. Also surrounded by plagioclase larger kyanite is overgrowing the white mica (Plate Fig. C). The kyanite is kinked by the S2 fabric. Staurolite forms small grains up to 0.5mm in diameter around garnet, associated with plagioclase. Only in some graphitic samples several millimeter large idiomorphic staurolite occurs in the matrix. White mica and a variable quartz content are the main components of the rock matrix. Several mica generations can be determined and verified by their chemical composition (Tab. 1). A fine grained paragonite-rich mica M1 (Pg₉₀Ms₈₋₁₀Ma₀₋₂, 3.05 Si p.f.u) forms the main schistosity S1. In the surrounding of the overgrowing kyanite-plagioclase aggregates the phengite component of the mica M2 (Ms₉₀Pg₁₀Ma₀, up to 6.44 Si p.f.u.) is increasing, whereas the paragonite component decreases. Additional unorientated mica M2 is overgrowing the schistosity S1. In some samples the phengite-rich M2 mica exsolves later on, into a muscovite M3 (Ms₉₀Pg₁₀Ma₀, 6.20 Si p.f.u.) and a rim of biotite with the same crystallographic orientation. Also in the axial planes of the crenulation cleavage (S2) this exsolution occurs during recrystallisation and postdates the deformation (Plate Fig. D). Plagioclase can be found as single crystals in pressure shadows around garnet and surrounding the kyanite of the matrix. The anorthite component (Ab₇₄₋₈₁An₂₆₋₁₉) is decreasing from core to rim. Biotite occurs together with plagioclase in the pressure shadows of the garnet, as small crystals formed by the breakdown of mica M2 and as porphyroblasts within the matrix. Chlorite is rarely found as a retrograde phase replacing the garnet.

Of special interest are amphibolites with paragonite coexisting with calcic amphibole. They further contain garnet, plagioclase (An₄₀), biotite, ilmenite, magnetite and apatite. The amphibole can be classified as a ferrotschermakite according to LEAKE (1978). Paragonite (Pg₉₀₋₉₃Ms₇₋₁₀Ma₀, 6.00 Si p.f.u.) forms flakes up to 3 mm in size. In contact to amphibole and plagioclase it is replaced by fine grained muscovite (Ms₈₂₋₈₅Pg₁₅₋₁₈Ma₀, 6.40 Si p.f.u.) and oligoclase (An₂₅) during decompression (Plate Fig. E).

The most likely garnet forming reaction in the metapelitic rocks of the Wölz Complex from the Ramingstein Window is Chl + Ms + Qtz = Grt + Bt + H₂O. The prograde meta-

Tab. 2: Representative analyses of minerals from the Wölz and Bundschuh Complex.

Sample	WC-P	WC-P	WC-B	WC-B	WC-B	WC-B	BC-P	BC-P	WC-P	WC-B	BC-P		WC-P	WC-P
	RSP81	RSP114	RS6/95	RS6/95	RS6/95	RS6/95	RSP35	RSP35	RSP81	RS6/95	RSP131	Sample	RSP114	RSP114
Mineral	mica M1	mica M2	Pa	Ma	Ms	Ms Mx	mica M2	mica M1	Bt Mx	Bt Mx	Bt Mx	Mineral	St _{center}	Ctd _{rim}
SiO ₂	47,41	49,13	46,78	32,26	49,25	49,30	48,56	47,34	37,71	36,22	37,97	SiO ₂	28,57	25,25
TiO ₂	0,12	0,31	0,04	0,22	0,42	0,49	0,37	0,54	1,86	1,04	1,84	TiO ₂	0,53	0,00
Al ₂ O ₃	38,48	31,77	41,38	48,43	34,31	33,36	31,79	34,22	18,40	20,29	18,35	Al ₂ O ₃	54,13	41,54
Cr ₂ O ₃	0,00	0,00	0,01	0,01	0,07	0,05	0,00	0,06	0,00	0,00	0,00	Cr ₂ O ₃	0,00	0,00
FeO	0,53	1,50	0,73	0,84	1,48	1,37	1,61	1,28	16,29	20,59	16,43	FeO	9,83	21,48
MnO	0,00	0,03	0,04	0,11	0,04	0,01	0,00	0,00	0,12	0,03	0,09	MnO	0,26	0,16
MgO	0,00	2,11	0,00	0,00	1,16	2,05	2,19	1,28	11,75	10,94	11,38	ZnO	2,57	0,00
CaO	0,28	0,00	0,92	11,47	0,00	0,03	0,00	0,02	0,00	0,00	0,28	MgO	1,54	4,58
Na ₂ O	6,80	0,80	6,39	0,97	0,50	1,49	0,59	0,77	0,39	0,30	0,22	CaO	0,00	0,00
K ₂ O	0,95	8,60	0,23	0,42	7,03	7,01	9,77	9,42	8,73	5,80	8,67	Na ₂ O	0,00	0,00
Total	94,57	94,25	96,52	94,73	94,26	95,16	94,88	94,93	95,25	95,21	95,23	K₂O	0,00	0,00
												Total	97,43	93,01
Si	3,05	3,26	2,94	2,15	3,23	3,26	3,23	3,13	2,80	2,71	2,82	Si	1,718	1,696
Al IV	0,95	0,74	1,06	1,85	0,77	0,75	0,77	0,87	1,20	1,29	1,18	Si	0,024	0,000
Al VI	1,97	1,75	2,01	1,96	1,88	1,80	1,72	1,80	0,42	0,50	0,43	Ti	3,837	3,289
Ti	0,01	0,02	0,00	0,01	0,02	0,02	0,02	0,03	0,10	0,06	0,10	Al	0,000	0,000
Cr	0,00	0,00	0,01	0,00	0,01	0,00	0,00	0,00	0,00	0,00	0,00	Cr	0,494	1,207
Fe	0,03	0,08	0,04	0,05	0,08	0,08	0,09	0,07	1,01	1,28	1,02	Mn	0,014	0,009
Mn	0,00	0,00	0,00	0,01	0,00	0,00	0,01	0,01	0,01	0,01	0,01	Mg	0,138	0,459
Mg	0,00	0,21	0,00	0,00	0,13	0,20	0,22	0,13	1,30	1,22	1,26	Ca	0,000	0,000
Ca	0,02	0,00	0,06	0,82	0,00	0,00	0,00	0,00	0,00	0,00	0,02	Zn	0,114	0,000
Na	0,85	0,10	0,88	0,13	0,07	0,19	0,08	0,10	0,06	0,06	0,03	Na	0,000	0,000
K	0,08	0,73	0,02	0,04	0,67	0,65	0,83	0,80	0,83	0,56	0,82	K	0,000	0,000
Sum	6,96	6,89	7,02	7,02	6,86	6,94	6,96	6,94	7,73	7,69	7,69	Sum	6,339	6,660
O	11,00	11,00	11,00	11,00	11,00	11,00	11,00	11,00	11,00	11,00	11,00	O	10,00	10,00
Ms	0,08	0,88	0,02	0,04	0,91	0,77	0,91	0,89	—	—	—			
Pa	0,89	0,12	0,92	0,13	0,09	0,23	0,08	0,11	—	—	—			
Ma	0,02	0,00	0,06	0,83	0,00	0,00	0,00	0,00	—	—	—			
Ann	—	—	—	—	—	—	—	—	0,44	0,51	0,45			
Phl	—	—	—	—	—	—	—	—	0,56	0,49	0,55			

Sample	WC-P	WC-P	WC-P	WC-P	WC-B	WC-B	WC-B	BC-P	BC-P		WC-P	WC-B	BC-P	BC-P
	RSP81	RSP81	RSP81	RSP81	RS6/96	RS6/96	RS6/96	RSP131	RSP131	Sample	RSP81	RS6/95	RSP131	RSP131
Mineral	center	—	Grt	rim	Grt _{core}	Grt _{rim}	Grt _{rim}	Grt _{core}	Grt _{rim}	Mineral	PI	PI	PI 1	PI 2
SiO ₂	36,96	37,20	37,35	37,65	37,52	38,28	38,11	37,01	37,17	SiO ₂	64,73	63,27	66,00	67,98
TiO ₂	0,17	0,11	0,15	0,08	0,10	0,10	0,02	0,04	0,06	TiO ₂	0,00	0,00	0,02	0,00
Al ₂ O ₃	20,90	20,77	20,96	21,17	22,07	21,14	21,88	21,41	21,55	Al ₂ O ₃	22,66	23,50	22,04	20,31
FeO	29,10	31,90	32,19	33,30	26,41	30,33	31,74	32,57	29,61	FeO	0,04	0,34	0,16	0,08
MnO	4,10	0,50	0,40	0,42	7,91	0,04	3,40	1,41	1,18	MgO	0,00	0,08	0,00	0,00
MgO	0,92	1,35	1,54	3,55	1,43	3,10	2,22	3,76	2,94	CaO	4,31	4,15	3,36	1,10
CaO	7,63	7,60	7,27	3,90	4,60	7,16	3,21	3,37	7,18	Na ₂ O	9,18	8,76	9,81	11,13
Total	99,78	99,43	99,86	100,1	100,04	100,15	100,58	99,57	99,69	K₂O	0,00	0,06	0,00	0,00
										Total	100,92	100,2	101,39	100,60
Si	2,99	3,00	3,00	3,00	3,01	3,02	3,01	2,97	2,97	Si	2,83	2,79	2,87	2,96
Al IV	0,01	0,00	0,00	0,00	0,00	0,00	0,00	0,03	0,04	Al	1,17	1,21	1,13	1,04
Al VI	1,98	1,98	1,99	1,99	2,01	1,98	2,01	1,99	1,99	Ti	0,00	0,00	0,00	0,00
Ti	0,01	0,01	0,01	0,01	0,00	0,01	0,01	0,00	0,00	Fe	0,00	0,01	0,01	0,00
Fe ³⁺	0,02	0,02	0,01	0,01	0,00	0,00	0,00	0,01	0,01	Mg	0,00	0,00	0,00	0,00
Fe ²⁺	1,95	2,14	2,16	2,21	2,19	2,00	1,81	2,17	1,96	Ca	0,20	0,20	0,16	0,05
Mn	0,28	0,03	0,03	0,03	0,24	0,01	0,58	0,10	0,08	Na	0,78	0,76	0,83	0,94
Mg	0,11	0,16	0,18	0,42	0,27	0,37	0,18	0,45	0,35	K	0,00	0,00	0,00	0,00
Ca	0,66	0,66	0,63	0,33	0,28	0,61	0,41	0,29	0,61	Sum	4,98	4,97	5,00	4,99
Sum	8,00	7,99	8,00	8,00	8,00	8,00	8,01	8,01	8,01	O	8,00	8,00	8,00	8,00
O	12,00	12,00	12,00	12,00	12,00	12,00	12,00	12,00	12,00					
alm	0,65	0,72	0,72	0,74	0,73	0,67	0,61	0,72	0,65	an	0,21	0,21	0,16	0,05
sps	0,09	0,01	0,01	0,01	0,08	0,00	0,19	0,03	0,03	ab	0,79	0,79	0,84	0,95
pyr	0,04	0,05	0,06	0,14	0,09	0,12	0,06	0,15	0,12	or	0,00	0,00	0,00	0,00
grs	0,21	0,21	0,20	0,11	0,09	0,20	0,14	0,09	0,20					
anr	0,01	0,01	0,01	0,01	0,00	0,00	0,00	0,01	0,01					

WC-P...Wölz Complex, Predlitz east of Ramingstein; WC-B...Wölz Complex, Bretstein valley; BC-P...Bundschuh Complex, Predlitz east of Ramingstein.

morphic path passed the chloritoid stability field. Later on staurolite replaced the chloritoid by the reaction $Ctd + Qtz = St + Grt + H_2O$. Peak metamorphic conditions are represented by staurolite and kyanite bearing assemblages just within the beginning of the stability of these minerals. It is evident, that both minerals are formed by paragonite consuming, plagioclase forming reactions: $Chl + Pg + Qtz = St + Pl + H_2O$ and $Pg + Qtz = Pl + Ky + H_2O$. HOINKES (1981) deduced a temperature of about 570 °C (at a pressure of 5 kbar) in similar assemblages of the Schneeberg Complex west of the Tauern Window. These temperatures fit with those determined by garnet-biotite thermometry using empirical methods (542-583 °C at 5.5 kbar, HODGES & SPEAR 1982) as well as the thermodynamic data-set of BERMAN (1988) in connection with the GEO-calc software (BERMAN et al. 1987: 540-570 °C in the range of 5.5-7 kbar). Peak pressure conditions in the Ramingstein Window can be estimated by the phengite-component of the M2 mica. Deduced from textural criteria this mica generation is a product of the kyanite forming, paragonite-consuming reaction. Pressure estimations by the phengite-barometry of MASSONNE & SCHREYER (1987) yielded 7 kbar (minimum pressure in case of lack of K-feldspar, estimated at 570 °C). These conditions are in agreement with the occurrence of equilibrium assemblages of paragonite coexisting with calcic amphibole, which represent rather restricted P-T conditions within the epidote-amphibolite facies (EVANS 1990). Paragonite amphibolites are indicators of high-pressure re-

gional metamorphism, close to, but still below the omphacite stability field in a mafic bulk system. They must be considered as direct precursors of low-pressure/high temperature eclogites in a regional metamorphic regime in a stability field of 7-10 kbar at 500-600 °C (KONZETT & HOINKES 1996, TEIML et al. in prep.).

Peak metamorphic conditions were reached syn- to postdeformativ with the development of the S1 schistosity, because kyanite and staurolite are kinked by the crenulation cleavage S2. P-T conditions after the metamorphic peak were calculated from $Grt + Bt + Pl + Ms$ (M3) which are in textural equilibrium in the pressure shadow of the garnet (SCHUSTER 1994). 550 °C and 5.5 kbar were deduced using the data-set of BERMAN (1988) in connection with the GEO-calc software (BERMAN et al. 1987).

The age of the metamorphic imprint of the Wölz Complex in the Ramingstein Window was determined by the Sm-Nd method. A garnet-garnet+ilmenite-WR isochron of a paragonite-bearing amphibolite yields 100.6 ± 6.3 Ma (Fig. 5A). This data represents the age of the high-pressure imprint. Garnet from a quartz and feldspar-rich metapelitic sample (Fig. 5B) shows a garnet-WR isochron age of 84 ± 6 Ma which is interpreted as the crystallisation age of the late-kinematic garnet. Several K-Ar (88-82 Ma) and Rb-Sr (74-78 Ma) cooling ages on muscovite and biotite respectively prove the Eoalpine age of metamorphism (SCHUSTER 1994) (Tab. 3).

The Sm-Nd data are well in line with ages from the eclogite-

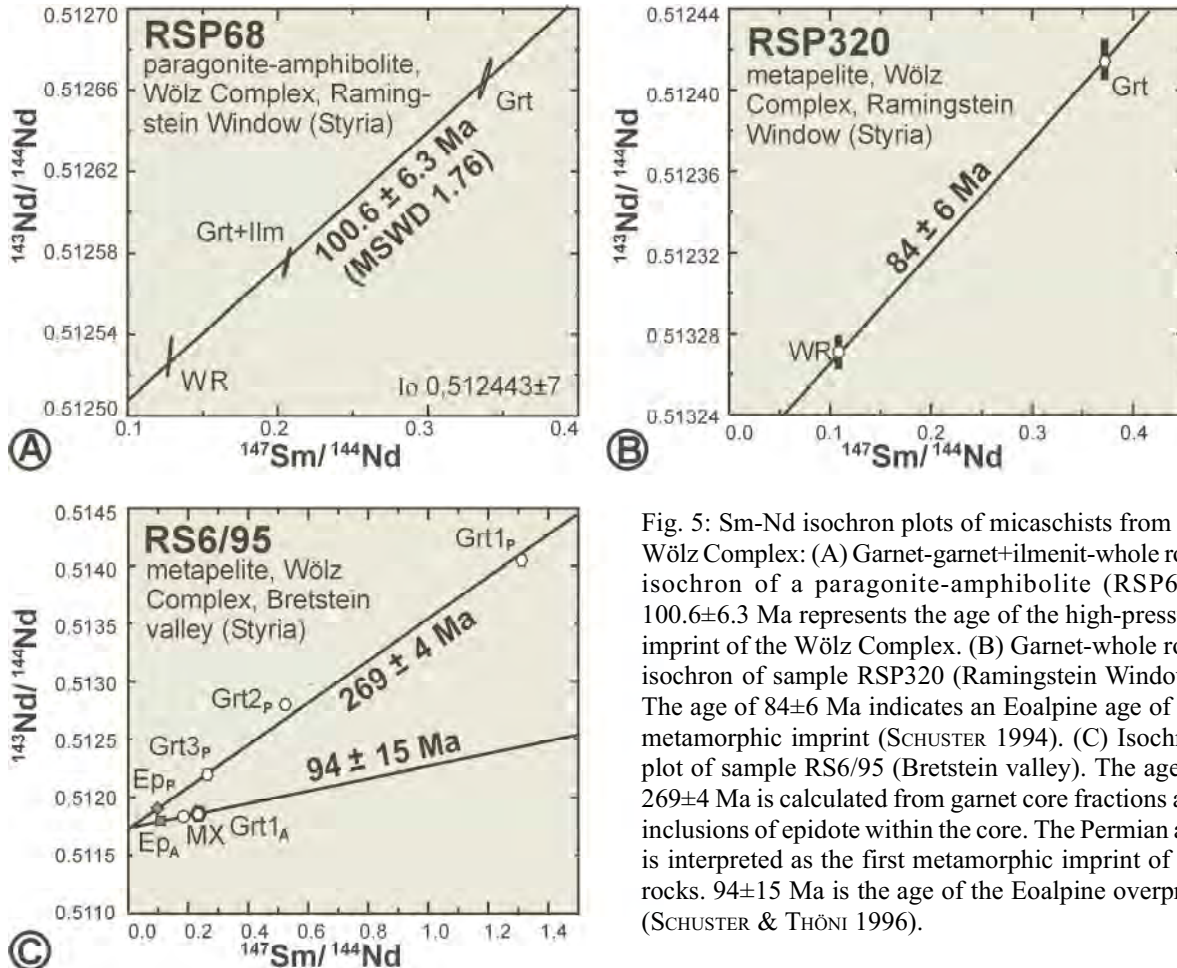


Fig. 5: Sm-Nd isochron plots of micaschists from the Wölz Complex: (A) Garnet-garnet+ilmenite-whole rock isochron of a paragonite-amphibolite (RSP68). 100.6 ± 6.3 Ma represents the age of the high-pressure imprint of the Wölz Complex. (B) Garnet-whole rock isochron of sample RSP320 (Ramingstein Window). The age of 84 ± 6 Ma indicates an Eoalpine age of the metamorphic imprint (SCHUSTER 1994). (C) Isochron plot of sample RS6/95 (Bretstein valley). The age of 269 ± 4 Ma is calculated from garnet core fractions and inclusions of epidote within the core. The Permian age is interpreted as the first metamorphic imprint of the rocks. 94 ± 15 Ma is the age of the Eoalpine overprint (SCHUSTER & THÖNI 1996).

Sample	Unit / Locality	Nd [ppm]	Sm [ppm]	¹⁴⁷ Sm/ ¹⁴⁴ Nd	¹⁴³ Nd/ ¹⁴⁴ Nd	2σm	Grt-Ep [Ma]	ε ₀ (Nd)	T Nd _{DM}
RS6/95 Mx	micaschist WC-B	20.14	6.28	0.1885	0.511966	± 7			
RSR6/95 Ep	epidote inclusion rim	158.9	29.01	0.1104	0.511917	± 12			
RSR6/95 Grt	garnet rim	5.006	1.961	0.2368	0.511995	± 8	94±15		
RS6/95 Ep	epidote inclusion core	1721	279.7	0.0982	0.511907	± 7			
RS6/95 Grt1	garnet (ultrapure)	1.114	2.426	1.3174	0.514053	± 16	268±2		
RS6/95 Grt2	garnet (high magnetic)	2.649	2.621	0.5981	0.512809	± 34			
RS6/95 Grt3	garnet (low magnetic)	7.076	3.190	0.2725	0.512190	± 9	261±6		
RSP320 WR	paragneiss WC-P	33.61	6.200	0.1132	0.512271	± 7		6.25	1.18
RSP320 Grt	garnet (ultrapure)	2.912	1.814	0.3806	0.512416	± 8	84±6		

Sample	Unit / Locality	Sr [ppm]	Rb [ppm]	⁸⁷ Rb/ ⁸⁶ Sr	⁸⁷ Sr/ ⁸⁶ Sr	2σm	Bt-WR [Ma]	Io	2σm	K-Ar [Ma]
RSP44WR	micaschist WC-P	242	217	2.6023	0.72003	± 8		0.717189	± 3	
RSP44Ms	muscovite	454	340	2.1767	0.72087	± 3				82±2
RSP44Bt	biotite	9.03	686	225.94	0.96383	± 35	76.8±0.66			84±3
RSP68WR	amphibolite WC-P	324	55.2	0.4936	0.71033	± 7		0.709812	± 4	
RSP68Ms	muscovite	647	181	0.8123	0.71102	± 5				
RSP68Bt	biotite	5.98	241	118.37	0.83406	± 25	73.9±0.74			
RSP86WR	amphibolite WC-P	387	41.1	0.3102	0.70729	± 6				
RSP86Ms	muscovite	1098	130	0.3445	0.70703	± 12				
RSP114WR	micaschist WC-P	70.8	199	8.1547	0.74739	± 5		0.738806	± 7	
RSP114Ms	muscovite	143	351	7.1374	0.74905	± 5				86±3
RSP114Bt	biotite	1.64	778	1604.5	2.42779	± 3	74.1±0.73			84±3
RSP127bWR	micaschist BC-P	148	109	2.1395	0.71955	± 7		0.717182	± 4	
RSP127bMs	muscovite	337	161	1.3876	0.71753	± 14				
RSP127bBt	biotite	3.94	327	247.73	0.99136	± 16	77.9±0.77			
RSP69Ms	muscovite WC-P									88±3
RSP113Ms	muscovite WC-P									83±3
RSP119Ms	muscovite WC-P									88±3

WC-P...Wölz Complex, Predlitz east of Ramingstein; WC-B...Wölz Complex, Bretstein valley; BC-P...Bundschuh Complex, Predlitz east of Ramingstein

Tab. 3: Sm-Nd, Rb-Sr and Ar-Ar isotopic data from the Wölz and Bundschuh Complex.

bearing series of the Saualm-Koraln Complex. Garnets from eclogites are in the range of 110-95 Ma whereas garnets from the metapelitic host rocks yielded 90-85 Ma (THÖNI 1999).

4.1.2. Polyphase assemblages from the eastern Wölz Complex

The area around Bretstein and Oberwölz has been investigated by SCHIMANA (1984), and by ABART & MARTINELLI (1991). Recent studies show that in this area two different units, both dominated by micaschists are present (SCHUSTER et al. 1999a, BERNHARD & HOINKES 1999). In this paper we only deal with the Wölz Complex, which is overlain by the Rappolt Complex (Fig. 3B). The polymetamorphic history of the Wölz Complex can be deduced from garnet crystals with distinct cores. The most frequent lithologies of this

area are paragneisses, micaschists and quartz-rich micaschists. Minor mica-bearing amphibolites and Permian pegmatites are outcropping (JÄGER & METZ 1971, SCHUSTER & THÖNI 1996).

In the Bretstein area micaschists containing polyphase, idiomorphic garnet crystals occur as scarce, up to 25 m thick concordant layers within micaschists and paragneisses with texturally single phase garnets. North of Oberwölz micaschists with polyphase garnets are dominating. The investigated lithologies show a matrix assemblage of garnet, muscovite, biotite, chlorite, albite, quartz and rutile. As in the western Wölz Complex the dominating schistosity (S1) has been overprinted by steeply dipping axial planes of the east-west orientated crenulation cleavage (S2).

Garnet shows two different morphological types. Individues of type one are polyphase crystals of 5 to 20 mm in diameter (Plate Fig. F) with an idiomorphic pinkish core (Grt_p) and a reddish rim (Grt_A). In the core monomineralic inclusions of

margarite, paragonite, muscovite, epidote, quartz, ilmenite and tourmaline occur whereas in the rim quartz, epidote, rutile and muscovite as the only mica are present. North of Oberwölz additionally staurolite and chloritoid can be observed within the inner part of the rim. The chemical zonation of the garnet crystals are characterised by a distinct break that fits exactly with the optical border between Grt_p and Grt_A (Fig. 5B). The cores (Grt_p) are chemically zoned with increasing FeO, MgO and X_{MgO}, decreasing MnO and a constant CaO content of about 4 wt%. The rims show much higher CaO (about 8 wt%), a slightly increasing MgO content and a much higher X_{MgO}. Type two garnets are reddish, optically and chemically unzoned and exhibit idiomorphic crystals of up to 6 mm in size. Inclusions are ilmenite, rutile, quartz, muscovite, epidote and tourmaline. Their chemistry is exactly the same as those of the Grt_A generation and argues for a contemporaneous formation. Determination of the P/T conditions during the growth of the garnet cores (Grt_p) is difficult due to the later overprint. However the existence of the three mica varieties margarite (Ma₈₃Pg₁₃Ms₄), paragonite (Pg₉₂Ms₆Ma₂) and muscovite (Ms₉₁Pg₉Ma₀, 6.40 Si p.f.u.) which occur as inclusions can be used for qualitative estimations. They form single crystals of up to 0,7 mm in diameter. It is presumed that the micas grew in equilibrium during prograde metamorphism before they were overgrown by the garnet core. Chemistry of the garnet does not change in the surrounding of the mica inclusions. Therefore the chemical composition was not influenced by the later overprint. The chemical composition of the micas are close to their end member compositions. In comparison with natural (FEENSTRA 1996, HÖCK 1974, OKUYAMA-KUSUNOSE 1985) and experimental data (FRANZ et al. 1977) this fact argues for a low-pressure metamorphism at greenschist facies conditions. From the presence of chlorite and the lack of staurolite in the rocks of the Bretstein valley upper greenschist facies conditions can be expected during the formation of the garnet generation Grt_A. Staurolite and chloritoid inclusions within Grt_A argue for lowermost amphibolite facies conditions in the area north of Oberwölz. Geochronological investigations yielded a Permian isochron age of 269±4 Ma for the garnet core (Grt_p) (Tab. 3; Fig 5C). Due to the used separation technique, ruling out a contamination of the core separate by the rim, and the fact that the sampled area experienced only greenschist facies conditions during the later overprint, clearly below the blocking-temperature for the Sm-Nd system in garnet (HENSEN & ZHOU 1995), the measured ages can be interpreted as formation ages of the garnet cores. The age of the garnet rim (Grt_A) was determined by analysis of a garnet-rim concentrate, inclusions of epidote inside the rim and a matrix powder. The result of 94±15 Ma defines the age of the Eoalpine overprint (SCHUSTER & THÖNI 1996).

4.1.3. Metamorphic zonation of the Wölz Complex

Until now no relics of a pre-Permian metamorphic imprint have been found in the Wölz Complex. Consequently this unit was characterised by garnet-free low-grade or weakly metamorphic rocks before. A Permian low-pressure(?) metamorphic event and contemporaneous pegmatite intrusions (SCHUSTER & THÖNI 1996) are visible in the eastern part of the investigated area (Fig. 6A). Scarce distinct cores within garnets from the southwestern Wölz Complex north of Spittal a.d. Drau might be related to the Permo-Triassic tectonothermal event.

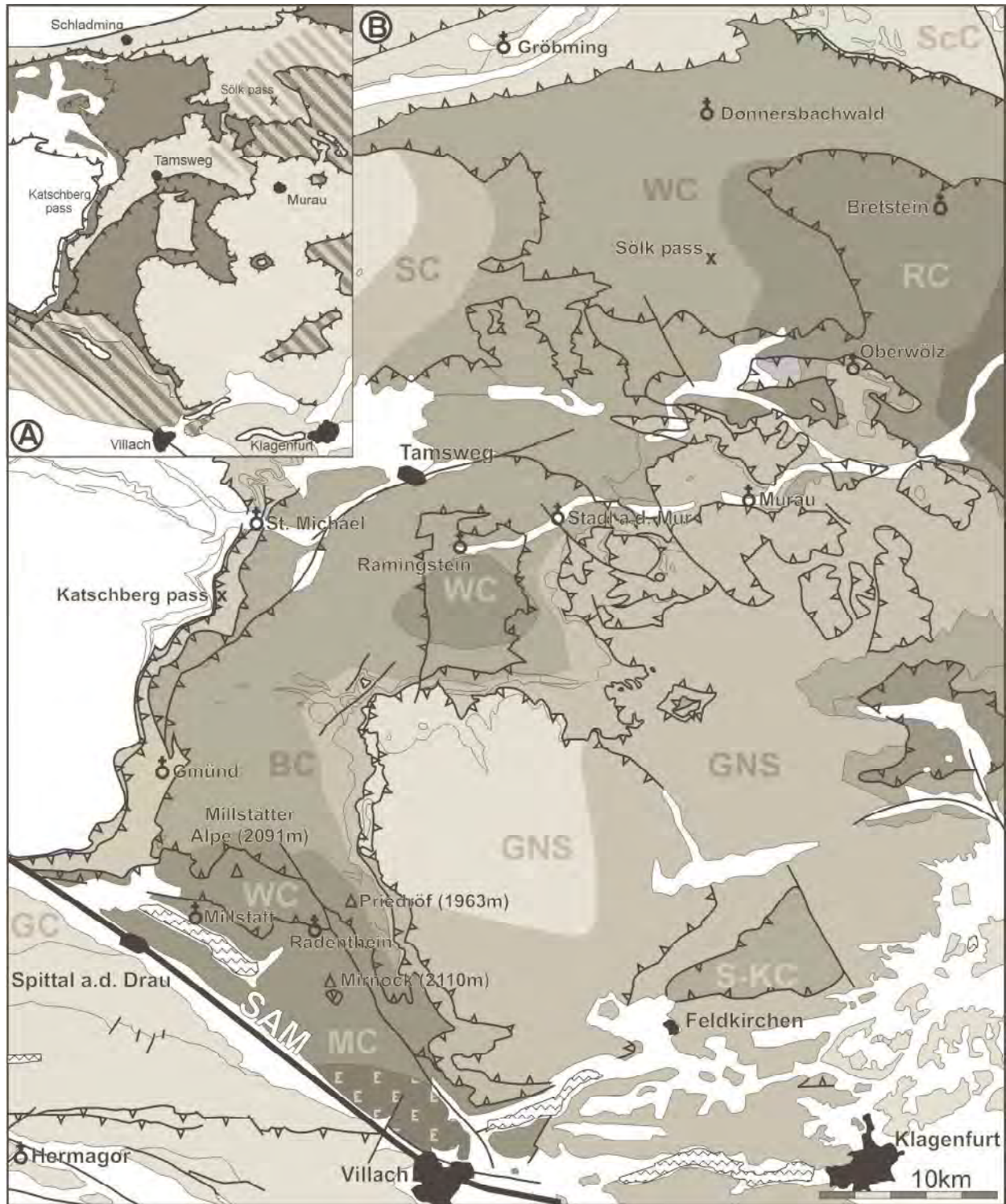
The Eoalpine metamorphic imprint of the Wölz Complex is characterised by a high-pressure event at c. 100 Ma and an isothermal decompression at about 90-85 Ma (TEIML et al. in prep.). This imprint shows a zonation with decreasing conditions from south to north (Fig. 6B). In the south Radenthein Complex medium-grade metamorphic conditions can be deduced by the textural equilibrium of garnet, staurolite and kyanite. Thermobarometric results yielded c. 600 °C at 10 kbar for metapelitic rocks (KOROKNAI et al. 1999) and about 590±20 °C at 7-8 bar for basic rocks (TEIML et al. in prep.). In the Ramingstein Window c. 570 °C and 7 kbar were determined for syn-deformational peak metamorphic conditions. Towards the north and the east there is a lack of thermobarometric data. However the principal distribution of the metamorphic grades can be deduced by the occurrence of index minerals. Staurolite and prograde staurolite breakdown by the reaction $St + Qtz = Grt + Ky + H_2O$ (ABART & MARTINELLI 1992) can be found north of Oberwölz. Towards the north the temperatures decrease to lower greenschist facies at the margin to the Greywacke Zone.

4.2. The Bundschuh Complex

The Bundschuh Complex overlies the Wölz Complex in the northwest of the Gurktal Nappe. Mapping showed that it is one continuous sheet which consists of fine-grained paragneisses with some intercalations of felsic biotite-free orthogneisses (SCHWINNER 1927: Priedröf paragneisses, Bundschuh orthogneisses) in the lower part, whereas micaschists and intercalated amphibolites are frequent in the upper part of the series, within the centre of a large scale gentle syncline structure (west of Gmünd). The Mesozoic Stangalm Unit transgresses unconformably onto this pre-Alpine syncline structure. Detailed descriptions of the lithologies are given in THURNER (1927), SCHIMANA (1986), THEINER (1987), EXNER (1990), SCHUSTER (1994) and KOROKNAI et al. (1999).

The Priedröf paragneisses contain the mineral assemblage garnet, biotite, plagioclase (albite and oligoclase), muscovite and quartz. In the micaschists additional staurolite, pseudo-

Fig. 6: Schematic distribution of metamorphic grade in the Austroalpine units east of the Tauern Window: (A) Pre-Alpine metamorphic imprint during the Hercynian- (370-310 Ma) and Permo-Triassic event (280-210 Ma). (B) Eoalpine metamorphic imprint at about 90 Ma (compiled from SCHIMANA 1984, SCHIMANA 1986, ABART & MARTINELLI 1991, SCHUSTER 1994). SAM = southern limit of Alpine Metamorphism (HOINKES et al. 1999).



(A) Map of pre-Alpine metamorphism

- post-Permian rocks
- pre-Permian unmetamorphic or low-grade metamorphic rocks with a Permo-Triassic low-grade metamorphic overprint
- ▨ Hercynian medium-grade metamorphic rocks with a Permo-Triassic medium to high-grade metamorphic overprint
- Hercynian low-grade metamorphic rocks
- ▨ Hercynian medium-grade metamorphic rocks

(B) Map of Eoalpine metamorphism

- Quaternary and Tertiary sediments, Pennine
- unmetamorphic and anchimetamorphic rocks
- lower greenschist facies metamorphic rocks (partly reset of the Ar-Ar isotopic system >350 °C)
- ▨ upper greenschist facies metamorphic rocks (garnet-in reactions >450 °C)
- ▨ lower amphibolite facies rocks (staurolite-in reactions >550 °C)
- ▨ upper amphibolite facies rocks (staurolite-out reactions >650 °C)
- ▨ eclogite facies rocks

morphs after staurolite and rarely chloritoid are present.

Garnets are very characteristic in the whole lower part of the unit. In the paragneisses they have an average grain-size of less than 0.5 mm, whereas in the micaschists they are up to 2 cm in diameter (Plate Fig. G). Optically an inclusion-rich (graphite, fluid inclusions?, quartz), often idiomorphic core (Grt_H) clearly can be distinguished from an inclusion-free rim (Grt_A). The cores are compositionally homogenous with low CaO contents of 3-5 wt% (Fig. 4B). In the rim the CaO content is much higher (6-8 wt%), FeO, MgO and also X_{MgO} are lower.

The occurrence of **staurolite** in the Bundschuh Complex is controlled by the whole rock chemistry (THEINER 1987). It occurs throughout in the micaschists, but is scarce in the paragneisses. Two generations of staurolite can be distinguished (SCHIMANA 1986). The older staurolite (St_H) is in textural equilibrium with the garnet cores Grt_H and forms crystals of up to 15mm in size, which are often partly or fully replaced by mica and chlorite. A younger staurolite generation (St_A) can be determined by its occurrence as small idiomorphic crystals within pseudomorphs after St_H . It can only be found in the lowermost part of the unit in contact to the underlying Radenthein Complex. **Chloritoid** appears within the pseudomorphs after staurolite in the upper part right up to the top of the unit. The **plagioclase** in the matrix of the Priedröf paragneisses is an oligoclase, whereas albite forms nodules and aggregates in equilibrium with the younger garnet generation (Grt_A). Additional small **potassium feldspar** crystals occur together with chlorite in the matrix and are most probably a product of the retrograde reaction $\text{Ms} + \text{Bt} = \text{Chl} + \text{K-feldspar}$.

Textures and zonation pattern of the garnet suggest that the Bundschuh Complex is polymetamorphic (Fig. 6A and 6B). The older assemblages characterised by garnet $\text{Grt}_H \pm \text{St}_H + \text{Pl}$ (oligoclase) + $\text{Bt} + \text{Ms} + \text{Qtz}$ were formed under amphibolite facies conditions. The flat element distribution patterns of the garnet Grt_H might be an indication for homogenisation (SCHIMANA 1986, THEINER 1987) at temperatures of more than 600 °C (e.g. YARDLEY 1977). A Hercynian age of this medium-grade event can be deduced from Rb-Sr ages (350-370 Ma) of mica in the Bundschuh orthogneisses (FRIMMEL 1987).

Geochronological data indicate an Eoalpine age for the overprinting event (SCHIMANA 1986, SCHUSTER 1994). Medium-grade peak metamorphic conditions of up to c. 620 °C and 12 kbar (KOROKNAI et al. 1999) were reached in the lowermost parts of the unit in the south, whereas most of the unit experienced a low-grade overprint. Below the Mesozoic cover the temperatures in the crystalline basement were less than 400 °C, because no Eoalpine rims developed around the Hercynian garnet cores and the K-Ar isotopic system of the Hercynian micas was only partly reset (SCHIMANA 1986).

4.3. The Bundschuh thrust

Taking into account that the Bundschuh Complex experienced a distinctly higher metamorphic grade in Hercynian times than the Wölz Complex, a tectonic superposition

of the Bundschuh Complex after the Hercynian metamorphic event can be deduced. The juxtaposition could have happened in late-Hercynian or during Eoalpine time. Petrological, tectonic and structural arguments support the second possibility:

- ⇒ The Hercynian garnets in the Bundschuh Complex are well preserved not only at the top of the unit, but also directly above the thrust plane. In this position they could have hardly survived if the Wölz Complex had been dehydrated during the Eoalpine metamorphism in its present day position from a low-grade to a medium-grade rock.
- ⇒ Para-autochthonous Mesozoic sediments are commonly overlying the Bundschuh Complex below the Gurktal Nappe, but not the Wölz Complex (Fig. 3B). If these two units already have been in contact since pre-Mesozoic times, they should have had the same Permo-Mesozoic sedimentary cover which must have been eroded selectively from the Wölz Complex later on. However, it is more likely that the two units were not transgressed by the same Mesozoic sediments and the tectonically higher portions of the Wölz Complex together with its cover series have been removed tectonically before the Bundschuh Complex and the Gurktal Nappe System were emplaced.
- ⇒ The pre-Alpine metamorphic history of the Wölz and Bundschuh Complex is strikingly different. A Permo-Triassic thermal imprint is a characteristic feature in the southern parts of the Austroalpine basement units east of the Tauern Window, e. g. in the former deeper levels of the Wölz Complex or the Sau-Koralmbau and Millstatt Complex (SCHUSTER et al. 1999a) (Fig. 6A). No indications for a Permo-Triassic thermal event have been found in the Bundschuh Complex. Therefore it is unlikely that the Bundschuh Complex was linked to the Wölz Complex in Permo-Triassic time.
- ⇒ The thrust zone itself is characterised by a sharp contact of the units and a broad mylonitic zone where the lithologies are fine grained but totally recrystallised. Mylonitisation and recrystallisation are Eoalpine in age: In the Wölz Complex syndeformativ inclusion trails in the center of garnets indicate a northwest-directed simple shear deformation during the time when the garnets started growing. Sometimes the garnets were broken during mylonitisation. However due to further growth all the individuals were recrystallised to idiomorphic crystal shapes again (Plate Fig. H). Now these garnets form elongated aggregates which give shear sense criteria for a top to northwest-directed deformation. In the Bundschuh Complex no unambiguous structures related to thrusting have been found. However in the lower part there are isoclinal, high temperature ductile folds which might be syndeformativ to the thrusting. The emplacement of the Bundschuh Complex is postdated by the development of the syn-D2 mega-fold of the Ramingstein Window which deforms the thrust plane (SCHUSTER 1994).

These arguments indicate a superposition of the Bundschuh Complex in Middle Cretaceous time during the west- to northwest-directed Eoalpine deformation D1, close before

the Eoalpine metamorphic peak conditions were reached. Accepting this the minimum transport distance can be estimated in the area around Radenthein. There the Wölz Complex is overthrust by the Bundschuh Complex from north of Villach in the southeast to the frame of the Tauern Window in the west over a distance of about 35 km (Fig. 3B).

5. Discussion

In this chapter the tectonic situation in the investigated area immediately east of the Tauern Window is discussed. After that the situation is compared to the area west of the Tauern Window and to a transect east of the Gurktal Nappe System. Generally a larger amount of shortening can be recognised from west to the east. Finally the pre-Alpine history of the Bundschuh Nappe and implications for Jurassic strike slip tectonics are discussed.

5.1. Comparison of sections through the Austroalpine basement units

East of the Tauern Window (Fig. 7A) the tectonically deepest part of the Austroalpine is the Lower Austroalpine represented by the frame of the Tauern Window and the Radstadt Nappe System. The polymetamorphic rocks of the overlying Schladming Complex experienced a Hercynian metamorphic imprint (HEJL 1984). During Eoalpine deformation this crystalline became to some extent ductil, but transgressive contacts with Permian sediments are still preserved (SLAPANSKY & FRANK 1987).

In the south the generally north dipping Millstatt Complex is characterised by the occurrence of marbles, Permian pegmatites and an Eoalpine eclogite facies metamorphic imprint (TEIML et al. in prep). At least during the Eoalpine exhumation it got in contact with the Wölz Complex, which is the overlying tectonic level. The Bundschuh Complex with

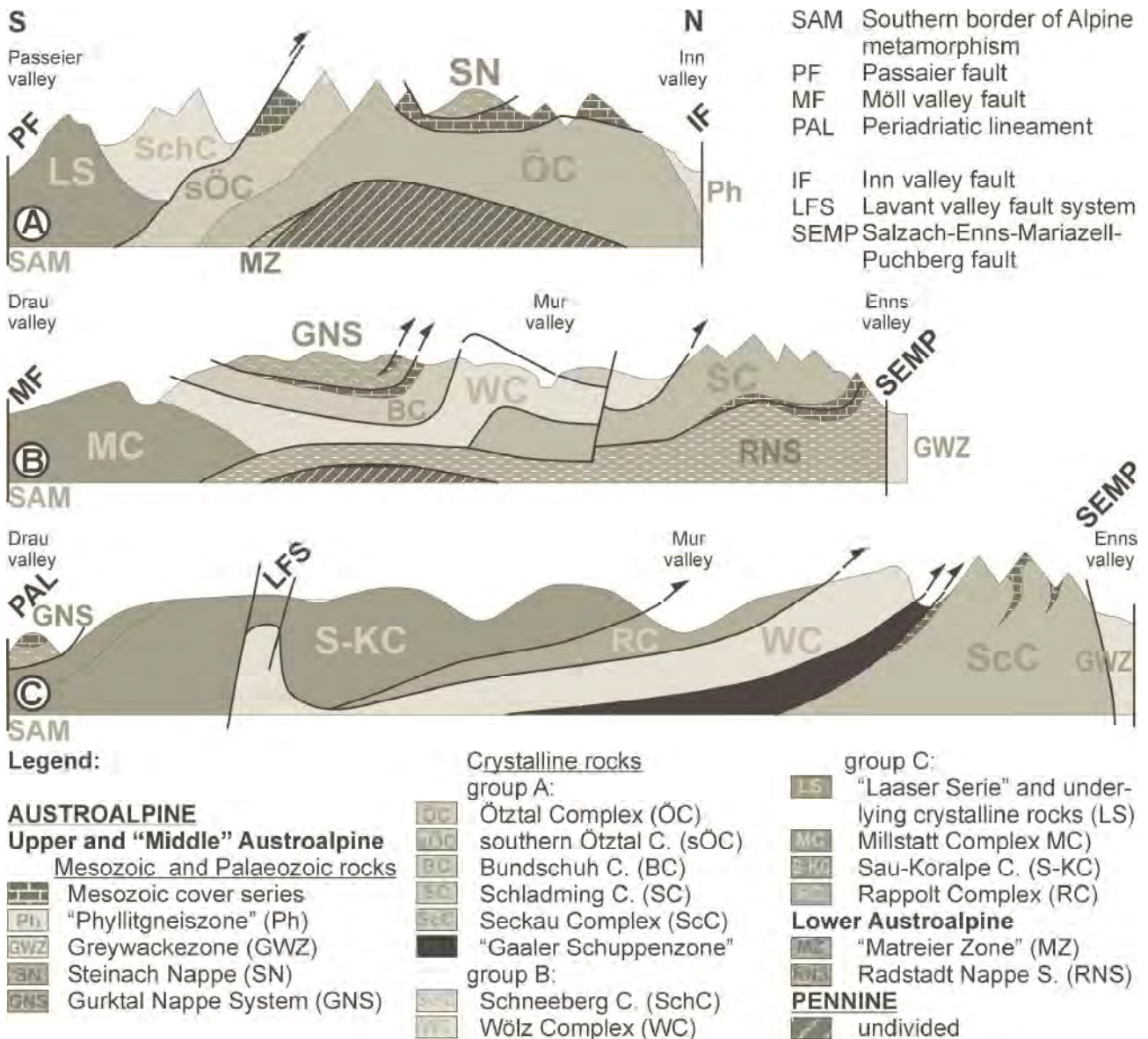


Fig. 7: Simplified cross sections through the Austroalpine units (A) west, (B) east of the Tauern Window and (C) east of the Gurktal Nappe System. Similar lithological units occur in different tectonic positions along the sections (explanation see text).

its Mesozoic cover took place on top of the western part of the Wölz Complex in Cretaceous time.

The uppermost tectonic unit of the area is the Gurktal Nappe System. Conglomerates of the Carboniferous Stangnock Formation (KRAINER 1993) within the Gurktal Nappe System show a specific and various petrographic composition along the outcrops at the northwestern border of the unit. Their pebble composition clearly depends on the lithology of the underlying units. E. g. in the Carboniferous Paal Conglomerate near Murau phyllites as in the Murau Nappe below are very abundant, whereas at Turrach close to the crystalline Bundschuh Complex ortho- and paragneiss boulders, up to 1 m in size occur. Based on petrological, chemical and geochronological investigations of these orthogneiss pebbles FRIMMEL (1987, 1988) was able to demonstrate that they were derived from the Bundschuh Complex. For that reason, the Gurktal Nappe System and the Bundschuh Complex must have already been neighbouring units during Carboniferous times (FRANK 1987, FRIMMEL 1988).

West of the Tauern Window comparable lithological units occur in a different tectonic arrangement (Fig. 7B). In the south the „Laaser Serie” and the partly Eoalpine eclogite-bearing lithologies below are dipping to the north. They typically contain Permian pegmatites and marbles and are very similar to the Millstatt Complex. The overlying Schneeberg Complex shows several striking similarities in lithology and metamorphism with the Wölz Complex northeast of Radenthein (PESCHL 1979, HOINKES 1981, SCHIMANA 1986). These units are juxtaposed onto the Ötztal Complex („Altkristallin”) in the north. The Ötztal Complex shows a Hercynian metamorphic imprint and an Eoalpine overprint which decreases northwards (THÖNI 1999). Its southern part is a lithological analogue to the Bundschuh Complex. To the north the Brenner Mesozoic forms the autochthonous cover of the Ötztal Complex and the Steinach Nappe holds the uppermost tectonic position. Carboniferous clastics very similar to that of the Gurktal Nappe System (KRAINER 1993) form a considerable portion of the Steinach Nappe. It is not possible to explain the different tectonic positions of the Bundschuh and Wölz Complex in comparison to the southern Ötztal Complex and Schneeberg Complex by movements in relation to the Tertiary exhumation of the Tauern Window. An interpretation of this situation is discussed in the next chapter.

East of the Gurktal Nappe System a different situation can be recognised, too (Fig. 7C). The Saualm-Koraln Complex forms the major tectonic element in the southern part. It contains marbles associated with Permian pegmatites and it is characterised by a well proved Eoalpine eclogite facies metamorphic imprint (THÖNI & JAGOUTZ 1992). Therefore it resembles to the Millstatt Complex. In the south these rock series carry a sequence of less metamorphic micaschists and the southeastern most part of the Gurktal Nappe System with a Mesozoic cover. However the Saualm-Koraln Complex is thrust north-directed onto Eoalpine less metamorphic units. These units are from top to the bottom the Rappolt Complex, the Wölz Complex, slices of the Speik Complex and the Seckau Complex. The latter experienced a Hercynian medium-grade imprint (SCHARBERT 1981), it is covered by Mesozoic sediments and can be compared to the Schladming

Complex.

5.2. The pre-Alpine palaeogeographic position of the Bundschuh Complex

The Bundschuh Complex with its characteristic lithology is a foreign element east of the Tauern Window, but shows similarities to the southern part of the Ötztal Complex, for example the lithology of the para- and orthogneisses, the age of the biotite-free orthogneisses and the garnet zonation patterns (PESCHL 1988, SCHUSTER 1994). The para-autochthonous Mesozoic sediments on top of the Bundschuh Complex and the Gurktal Nappe System exhibiting clastic influence in the Anisian carbonates have often been compared with the Mesozoic cover series west of the Tauern Window (BECHSTÄDT 1978). At present we are still not able to reconstruct the pre-Alpine position of the Bundschuh Complex and the Gurktal Nappe System in detail. However, we assume their palaeogeographic position in the vicinity of the southern Ötztal Complex.

If the Bundschuh Complex and its Mesozoic cover, as well as the Gurktal Nappe System were originally situated further in the west, the question arises, how these units were transported to their present day position. A two-step transport is envisaged:

1. The second step, their emplacement onto the Wölz and Saualm-Koraln Complexes can be explained by the synmetamorphic, west- to northwest directed major superposed tectonic (D1) in Middle Cretaceous times. The following north directed deformation (D2) and the southeast directed Cretaceous to Tertiary extension (D3) caused only minor relative movements of the units.
2. The earlier tectonic processes, responsible for the transport of the units to the east, are confined as a system of steep sinistral strike slip faults. Largely obliterated by the later Alpine tectonics there is no chance for any direct dating of the strike slip zone.

The time of these strike slip movements is difficult to assess. Obviously they were active prior to Cretaceous tectonics and metamorphism, including the high-pressure event at c. 100 Ma (THÖNI 1999). The lower time limit is defined by the Triassic facies distribution (HAAS et al. 1995) (Fig. 8A). Therefore a Jurassic age is the most realistic assumption. Several indications argue for Jurassic sinistral strike slip tectonics:

- Jurassic sinistral strike slip faults are known from the European continent (ZIEGLER 1988) and are related to the opening of the North Atlantic and Penninic Ocean.
- Facies reconstructions for the Permo-Triassic sedimentary sequences indicate a zone of former westerly positioned tectonic units north of the Periadriatic line (HAAS et al. 1995). This zone consists of parts of the Defregger Alps, the Drauzug Unit, the Bundschuh Complex, the Gurktal Nappe System and the Transdanubian Range (KÁZMÉR & KOVÁCS 1985, HAAS et al. 1995). At present it is bordered by the Jaufen line (SPIESS 1995), the DAV (Deffregger-Antholz-Vals fault), the Bundschuh thrust and the Raba line in the north, by the

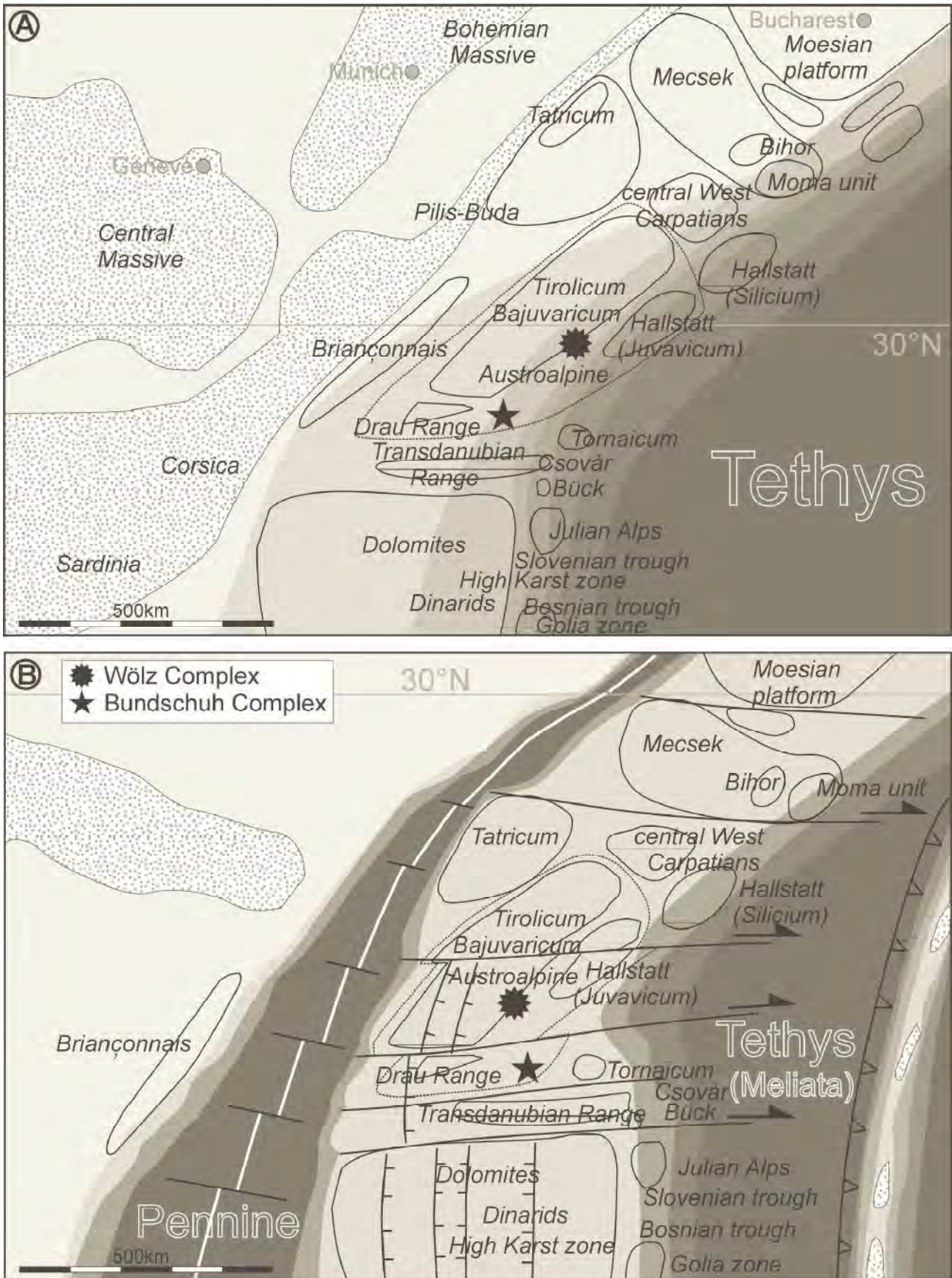


Fig. 8: Simplified palaeogeographic reconstructions of the western Tethys: (A) reconstruction of the late Triassic arrangement modified from HAAS et al. (1995). (B) Jurassic situation modified from GAWLICK et al. (1999). Sinistral strike slip faults are crosscutting through the Austroalpine. The rearrangement of the crustal blocks at the passive continental margin of the Tethys starts.

Periadriatic line and the Balaton line in the south. Shear zone activity of the original fault system might have been polyphase and has to be Jurassic to Lower Cretaceous in age, because the Upper Triassic Hauptdolomit-facies in the Drauzug and the Gurktal Nappe System implies a still westerly position of these units until Rhaetian time (BECHSTÄDT 1978, HAAS et al. 1995).

- Additional arguments for tectonic movements during Jurassic time are the occurrence of scarce crystalline pebbles within pelagic limestones of Jurassic age (LANTSCHNER et al. 1994) and the huge masses of Jurassic mega-breccias within the Northern Calcareous Alps (RISAVY 1996, SCHIEL 1995). Both observations argue for a relief which might have been caused by flower structures and pull apart basins along curved strike slip faults.

5.3. The sedimentary cover of the „Middle Austroalpine“

If the Bundschuh Complex and the Gurktal Nappe System have been located in the west prior to the Eoalpine collision another consequence arises: There remain no more Middle Austroalpine Mesozoic sediments on top of the Austroalpine crystalline basement units east of the Tauern Window, except at its northern margin. The vast areas of basement units in the south (e. g. Wölz or Saualpe-Koralpe Complex) are characterised by the Permo-Triassic high-temperature/low-pressure imprint (SCHUSTER et al. 1999b) which is related to crustal extension. Crustal blocks with the observed thermal characteristics will show subsidence over long time periods. During extension the subsidence is induced by the isostatic relaxation of the area, after that cooling of the basement to the relaxed geotherm will lead to a rise in density and again the result is subsidence. Most probable these crystalline units represent the basement on top of which large parts of the Northern Calcareous Alps (Tirolicum and Juvavicum) have been deposited. Accepting this, major parts of the Middle Austroalpine have been the basement on which the Upper Austroalpine Northern Calcareous Alps were deposited (Fig. 1B). This contradicts the definition of TOLLMANN (1959) who defined them as lateral neighbouring areas (Fig. 1A). Forty years ago, when TOLLMANN established his model it was a big step forward in understanding the geology of the Eastern Alps. It was in fully agreement with the state of the art. However, at present we should avoid the term “Middle Austroalpine” because in its sense it is more genetic than regional.

5.4. Jurassic tectonics

The emplacement of the Juvavic tectonic element during the Upper Jurassic, derived from the southeastern area of the Northern Calcareous Alps, is now a well established concept (LEIN 1987, MANDL 1984). Although the overall structural framework of this process is still poorly understood. A fundamental structural reorganisation at the border zone between the Northern Calcareous Alps and the Tethys ocean (Meliatia ocean) is a necessary consequence. It will

of course also affect the basement of the Mesozoic sediments.

Based on the palinspastic reconstruction of HAAS et al. (1995) for the facies arrangement in Triassic time (Fig. 8A) we speculate that during the opening of the Penninic realm, possibly wider in the Ligurian segment compared to the Tauern region, sinistral transpressive structures developed within the Austroalpine. Such structures are shown in an oversimplified manner in Fig. 8B. This process may be the beginning of the fundamental rearrangement of the crustal blocks forming the Tethyan passive continental margin until Lower – Middle Jurassic times (Fig. 8A). The Jurassic palaeogeographic and tectonic evolution in the addressed region is of fundamental importance for understanding the present day situation. However it is poorly understood and the discussion of this complex process is definitely beyond the scope of this paper.

Acknowledgements

This work has been supported by the *Fonds zur Förderung der wissenschaftlichen Forschung* (Project No. S47-GEO and P12277-GEO). We thank M. Jelenc for her help with the Rb-Sr isotope analyses and we are grateful to M. Thöni, S. Scharbert, H. Frimmel and K. Schmidt for discussion and reviewing the manuscript.

References

- ABART, R. & MARTINELLI, W. (1991): Variszische und alpidische Entwicklungsgeschichte des Wölzer Kristallins (Steiermark/Österreich). - Mitt. Ges. Geol. Bergbaustud. Österr., **37**: 1-14, Wien.
- BECHSTÄDT, TH. (1978): Faziesanalyse permischer und triadischer Sedimente des Drauzuges als Hinweis auf eine großräumige Lateralverschiebung innerhalb des Ostalpins. - Jb. Geol. B.-A., **121**: 1-121, Wien.
- BELOCKY, R. (1987): Strukturgeologische Untersuchungen in Kristallin und Gurktaler Decke im Raum Radenthein-Bad Kleinkirchheim (Nockgebiet/Kärnten/Österreich). - Unveröffentl. Diplomarbeit Formal-Naturwiss. Fak. Univ. Wien, 1-133, Wien.
- BERMAN, R.G., BROWN, T.H. & PERKINS, E.H. (1987): GEO-CALC: software for calculation and display of pressure-temperature-composition phase diagrams. - Mineral. Soc. Am., **72**: 861-862, Washington.
- BERMAN, R.G. (1988): Internally-consistent thermodynamic data for minerals in the system Na₂O-K₂O-CaO-MgO-Fe₂O₃-Al₂O₃-SiO₂-TiO₂-H₂O-CO₂. - J. Petrol., **29**: 445-522, Oxford.
- BERNHARD, F. & HOINKES, G. (1999): Polyphase micaschists of the central Wölzer Tauern. - Ber. Mineral. Ges., Beih. z. Eur. J. Mineral., **11/1**: 32, Stuttgart.
- CLAR, E. (1965): Zum Bewegungsbild des Gebirgsbaues der Ostalpen. - Verh. Geol. B. -A., **Sdh. G**: 11-35, Wien.
- DALLMEYER, R.D., NEUBAUER, F., HANDLER, R., MÜLLER, W., FRITZ, H., ANTONITSCH, W. & HERMANN, S. (1992): ⁴⁰Ar/³⁹Ar and Rb/Sr mineral age control for the pre-Alpine and Alpine tectonic evolution of the Austro-Alpine Nappe Complex, Eastern Alps. - ALCAPA-Field Guide 1992, 47-60, Graz.
- EVANS, B.W. (1990): Phase relations of epidote-blueschist. - Lithos, **25/1-3**: 3-23, Amsterdam.
- EXNER, CH. (1990): Erläuterungen zur Geologischen Karte des mittleren Lungaus. - Mitt. Ges. Geol. Bergbaustud. Österr., **36**:

- 1-38, Wien.
- FEENSTRA, A. (1996): An EMP and TEM-AEM Study of margarite, muscovite and paragonite in polymetamorphic metabauxites of Naxos (Cyclades, Greece) and the implications of fine mica interlayering and multiple mica generations. - *J. of Petrology*, **37**: 201-233, Oxford.
- FRIMMEL, H. (1987): Isotopengeologische Hinweise für die paläogeographische Nachbarschaft von Gurktaler Decke (Oberostalpin) und dem Altkristallin östlich der Hohen Tauern (Österreich). - *Schweiz. Mineral. Petrogr. Mitt.*, **66**: 193-208, Zürich.
- FRIMMEL, H. (1988): Metagranitoide am Westrand der Gurktaler Decke (Oberostalpin) - Genese und paläotektonische Implikationen. - *Jb. Geol. B.-A.*, **131**: 575-592, Wien.
- FRANK, W. (1987): Evolution of the Austroalpine Elements in the Cretaceous. - (In: FLÜGEL, H. W. & FAUPL, P. (Eds.): *Geodynamics of the Eastern Alps*), 379-406, (Deuticke) Wien.
- FRANK, W., ESTERLUS, E., FREY, I., JUNG, G., KROHE, A. & WEBER, J. (1983): Die Entwicklungsgeschichte von Stub- und Koralmkristallin und die Beziehung zum Grazer Paläozoikum. - *Jber. 1982 Hochschulschwerpkt*, **S15**: 263-293, Graz.
- FRANZ, G., HINRICHSEN, T. & WANNEMACHER, E. (1977): Determination of the miscibility gap on the solid solution series paragonite-margarite by means of infrared spectrometry. - *Contrib. Mineral. Petrol.*, **59**: 307-316, Heidelberg New York.
- FRÖITZHEIM, N., SCHMID, S.M. & FREY, M. (1996): Mesozoic paleogeography and the timing of eclogitfacies metamorphism in the Alps: A working hypothesis. - *Eclogae geol. Helv.*, **89**/1: 81-110, Basel.
- GAWLICK, H.J., KRYSSTYN, L., LEIN, R. & MANDL, G.W. (1999): Tectonostratigraphic concept for the Juvavic Domain. - *Tübinger Geowiss. Arb., Serie A*, **52**: 95-104, Tübingen.
- GENSER, J. & NEUBAUER, F. (1989) Architektur und Kinematik der östlichen Zentralalpen - eine Übersicht. - *Mitt. Naturwiss. Ver. Steiermark*, **120**: 203-219, Graz.
- HAAS, J., KOVÁCS, S., KRYSSTYN, L. & LEIN, R. (1995): Significance of Late Permian-Triassic facies zones in terrane reconstructions in the Alpine-North Pannonian domain. - *Tectonophysics*, **242**: 19-40, Amsterdam.
- HEIL, E. (1984): Geochronologische und petrologische Beiträge zur Gesteinsmetamorphose der Schladminger Tauern. - *Mitt. Ges. Geol. Bergbaustud. Österr.*, **30/31**: 289-318, Wien.
- HENSEN, B.J. & ZHOU, B. (1995): Retention of isotopic memory in garnets partially broken down during an overprint granulite-facies metamorphism: Implications for the Sm-Nd closure temperature. - *Geology*, **23/3**: 225-228, Boulder.
- HÖCK, V. (1974): Coexisting phengite, paragonite and margarite in metasediments of the Mittlere Hohe Tauern, Austria. - *Contrib. Mineral. Petrol.*, **43**: 261-273, Heidelberg New York.
- HODGES, K.V. & SPEAR, F.S. (1982): Geothermometry, geobarometry and the Al₂SiO₅ triple point at Mt. Moosilauke, New Hampshire. - *Am. Mineral.*, **67**: 1118-1134, Washington.
- HOINKES, G. (1981): Mineralreaktionen und Metamorphosebedingungen in Metapeliten des westlichen Schneeberger Zuges und des angrenzenden Altkristallins (Ötztaler Alpen). - *Tschermaks Min. Petr. Mitt.*, **28**: 31-54, Wien.
- HOINKES, G., KOLLER, F., RANTITSCH, G., DACHS, E., HÖCK, V., NEUBAUER, F. & SCHUSTER, R. (1999): Alpine metamorphism of the Eastern Alps. - *Schweiz. Mineral. Petrogr. Mitt.*, **79**/1: 155-181, Zürich.
- JÄGER, E. & METZ, K. (1971): Das Alter der Pegmatite des Raumes Bretstein-Pusterwald (Wölzer Tauern, Steiermark). - *Schweiz. Miner. Petrogr. Mitt.* **51**: 411-414, Zürich.
- KÁZMÉR, M. & KOVÁCS, S. (1985): Permian- Paleogene paleogeography along the eastern part of the Insubric-Periadriatic lineament system: evidence for continental escape of the Bakony-Drauzug Unit. - *Acta. Geol. Hung.*, **28**/1-2:71-84, Budapest.
- KONZETT, J. & HOINKES, G. (1996): Paragonite-hornblende assemblages and their petrological significance: an example from the Austroalpine Schneeberg Complex, Southern Tyrol, Italy. - *J. metamorphic Geol.*, **14**: 85-101, Oxford.
- KOROKNAI, B., NEUBAUER, F., GENSER, J. & TOPA, D. (1999): Metamorphic and tectonic evolution of Austroalpine units at the western margin of the Gurktal nappe complex, Eastern Alps. - *Schweiz. Mineral. Petrogr. Mitt.*, **79**: 277-295, Zürich.
- KRAINER, K. (1993): Late- and Post-Variscian Sediments of the Eastern and Southern Alps. - (In: NEUBAUER, F. & RAUMER, J.F. (Eds.): *The pre- Mesozoic Geology of the Alps*), 537-564, (Springer) Berlin Heidelberg New York.
- LANTSCHNER, M., LEIN, R. & THÖNI, M. (1994): Kristallingerölle in Liasbuntkalken der Lechtaler Alpen. - *Mitt. Ges. Geol. Bergbaustud. Österr.*, **39**: 211-220, Wien.
- LEAKE, B.E. (1978): Nomenclature of amphiboles. - *Am. Mineralogist*, **63**/11-12: 1023-1052, Washington.
- LEIN, R. (1987): Evolution of the Northern Calcareous Alps. - (In: FLÜGEL, H. W. & FAUPL, P. (Eds.): *Geodynamics of the Eastern Alps*), 85-102, (Deuticke) Wien.
- LOOMIS, T.P. & NIMICK, F.B. (1982): Equilibrium in Mn-Fe-Mg aluminous pelitic compositions and the equilibrium growth of garnet. - *Can. Mineralogist*, **20**: 393-410, Ottawa.
- MANDL, G.W. (1984): Zur Tektonik der westlichen Dachsteindecke und ihres Hallstätter Rahmens (Nördliche Kalkalpen, Österreich). - *Mitt. Österr. Geol. Ges.* **77**: 1-31, Wien.
- MASSONNE, H.J. & SCHREYER, W. (1987): Phengite geobarometry based on the assemblage with K-Feldspar, phlogopite, and quartz. - *Contrib. Mineral. Petrol.* **96**: 212-224, Heidelberg New York.
- MORAU, W. (1980): Die permische Differenzierung und die alpidische Metamorphose des Granitgneises von Wolfsberg, Koralle, SE-Ostalpen, mit Rb/Sr- und K/Ar-Isotopenbestimmungen. - *Tschermaks Mineral. Petrogr. Mitt.*, **27**: 169-185, Wien.
- NOWAK, H.W. (1986): Kristallisations und Deformationsgeschichte am S-Rand der Gurktaler Decke (Ostalpen, Kärnten). - *Unveröffentl. Diss. Formal-Naturwiss. Fak Univ Wien*, 1-173, Wien.
- OKUYAMA-KUSUNOSE, Y. (1985): Margarite-paragonite-muscovite assemblages from the low-grade metapelites of the Tono metamorphic aureole, Kitakama Mountains, Northeast Japan. - *J. Japanese Association Mineralogy Petrology Economic Geology*, **80**: 515-525, Tokyo.
- PESCHL, R. (1979): Geologische Entwicklungsgeschichte des Schneebergerzuges und der Laaser Serie im Timmelsjoch-Querschnitt. (Oberes Passeiertal, Südtirol. Italien). - *Unveröffentl. Diss. Formal-Naturwiss. Fak. Univ. Wien*, 1-98, Wien.
- PISTOTNIK, J. (1996): Geologische Karte der Republik Österreich 1: 50.000, Blatt 183 Radenthein. - (Geol. B.-A.) Wien.
- RATSCHBACHER, L. (1986): Kinematics of Austroalpine Cover Nappes. - *Tectonophysics*, **125**: 335-356, Amsterdam.
- RISAVY, R. (1996): Geologie und Fazies des Raumes Triebnitz-Pötschberg, steirische Kalkalpen, Salzatal (Österreich). - *Unveröffentl. Dipl.-Arb., Formal-Naturwiss. Fak. Univ. Wien*, 1-118, Wien.
- SCHARBERT, S. (1981): Untersuchungen zum Alter des Seckauer Kristallins. - *Mitt. Ges. Geol. Bergbaustud. Österr.*, **27**: 173-188, Wien.
- SCHIEL, B. (1995): Geologie und Fazies des Raumes Dürradmer-Greith, Salzatal, Steiermark (Österreich). - *Unveröffentl. Dipl.-Arb., Formal-Naturwiss. Fak. Univ. Wien*, 1-108, Wien.
- SCHIMANA, R. (1984): Strukturuntersuchungen in den Wölzer Glimmerschiefern am Ostrand der Wölzer Tauern. - *Unveröffentl. Vorarbeit Geol. Inst. Univ. Wien*, 1-75, Wien.
- SCHIMANA, R. (1986): Geologische Entwicklung des Kristallins in der Umgebung von Radenthein (Nockgebirge/Kärnten). - *Unveröffentl. Diss. Formal-Naturwiss. Fak. Univ. Wien*, 1-172, Wien.
- SCHUSTER, R. (1994): Die alpine Großüberschiebung an der Basis des Bundschuhkristallins (Steiermark/Kärnten/Salzburg). - *Unveröffentl. Dipl.-Arb. Formal-Naturwiss. Fak. Univ. Wien*, 1-120, Wien.
- SCHUSTER, R. & THÖNI, M. (1996): Permian Garnet: Indications for a regional Permian metamorphism in the southern part of the Austroalpine basement units. - *Mitt. Österr. Mineral. Ges.*, **141**: 219-221, Wien.

- SCHUSTER, R., HOINKES, G., KAINDL, R., KOLLER, F., LEBER, T., PUHL, J. & BERNHARD, F. (1999a): Metamorphism at the eastern end of the Alps - Alpine, Permo-Triassic, Variscan? - *Berichte der Deutschen Mineralogischen Gesellschaft, Beih. z. Eur. J. Mineral.*, **11/2**: 111-136, Stuttgart.
- SCHUSTER, R., SCHARBERT, S. & ABART, R. (1999b): Permo-Triassic crustal extension during opening of the Neotethyan ocean in the Austroalpine-South Alpine realm. - *Tübinger Geowissenschaftliche Arbeiten, Serie A*, **52**: 5-6, Tübingen.
- SCHWINNER, R. (1927): Der Bau des Gebirges östlich von der Lieser (Kärnten). - *Sitzungsber. mathem-naturwiss. Kl. Ak. Wiss. Abt. I*, **136**: 333-382, Wien.
- SLAPANSKY, P. & FRANK, W. (1987): Structural Evolution and Geochronology of the Northern Margin of the Austroalpine in the Northwestern Schladming Crystalline (NE Radstädter Tauern). - (In: FLÜGEL, H.W. & FAUPL, P. (Eds.): *Geodynamics of the Eastern Alps*), 244-262, (Deuticke) Wien.
- SPIESS, R. (1995): The Passeier-Jaufen Line: a tectonic boundary between Variscian and Eo-Alpine Meran-Mauls basement. - *Schweiz. Mineral. Petrogr. Mitt.*, **75**: 413-425, Zürich.
- TEIML, X., HOINKES, G. & SCHUSTER, R. (in prep.): Epidote-Amphibolite- and Eclogite-facies metamorphism of metabasites of the Austroalpine Millstatt and Radenthein Complex (Carinthia, Austria).
- THEINER, U. (1987): Das Kristallin der NW-Nockberge. Eine kristallingeologische Neuuntersuchung. - Unveröffentl. Diss. For- mal-Naturwiss. Fak. Univ. Wien, 1-154, Wien.
- THÖNI, M. & JAGOUTZ, E. (1992): Some new aspects of dating eclogites in orogenic belts: Sm-Nd, Rb-Sr and Pb-Pb isotopic results from the Austroalpine Saualpe and Koralpe type-locality (Carinthia/Styria, southeastern Austria). - *Geochim. Cosmochim. Acta*, **56**: 347-368, Oxford.
- THÖNI, M. (1999): A review of geochronological data from the Eastern Alps. - *Schweiz. Mineral. Petrogr. Mitt.*, **79/1**: 209-230, Zürich.
- TURNER, A. (1958): Erläuterungen zur geologischen Karte Stadl-Murau. - 1-106, (Geol. B.-A.) Wien.
- TOLLMANN, A. (1959): Der Deckenbau der Ostalpen auf Grund der Neuuntersuchung des zentralalpiner Mesozoikums. - *Mitt. Ges. Geol. Bergbaustud.*, **10**: 3-62, Wien.
- TOLLMANN, A. (1965): Faziesanalyse der alpidischen Serien der Ostalpen. - *Verh. Geol. B.-A.*, **Sdh. G**, 103-133, Wien.
- TOLLMANN, A. (1975): Die Bedeutung des Stangalm-Mesozoikums in Kärnten für die Neugliederung des Oberostalpins in den Ostalpen. - *N.Jb. Geol. Paläont. Abhandlungen*, **150/1**: 19-43, Stuttgart.
- TOLLMANN, A. (1977): *Geologie von Österreich Bd. I. Die Zentralalpen*. - 1-766, (Deuticke) Wien.
- YARDLEY, B.W.D. (1977): An empirical study of diffusion in garnet. - *Am. Mineral.*, **62**: 793-800, Washington.
- ZIEGLER, P. (1988): Evolution of the Arctic-North Atlantic and the Western Tethys. - *Am. Assoc. Pet. Geol. Mem.*, **43**: 1-197, Tulsa.

Plate

- A) Late-kinematic Eoalpine garnet (Grt_A) from a quartz and feldspar-rich gneiss. Crystal growth is syn- to postdeformative to the formation of the schistosity (S1) (RSP320; Wölz Complex, Ramingstein Window; parallel Nicols).
- B) Eoalpine garnet (Grt_A) within a mica-rich matrix. The porphyroblast was overgrowing the continuous schistosity (S1) in a plain strain regime. Inclusions of idiomorphic chloritoid (Ctd) crystals are orientated parallel to S1. At the edges of the garnet porphyroblasts kyanite (Ky) and staurolite (St) occur within the matrix (RSP114; Wölz Complex, Ramingstein Window; parallel Nicols).
- C) Kyanite (Ky) and albite (Pl) overgrowing paragonitic white mica (M1) by the reaction paragonite + quartz = kyanite + albite + H_2O . This reaction represents Eoalpine peak metamorphic conditions of the rock. The kyanite is overgrowing the main schistosity (S1) and is kinked by the crenulation cleavage (S2) (RSP81; Wölz Complex, Ramingstein Window; parallel Nicols).
- D) Exsolution of phengitic mica (M2) to biotite and muscovite (M3). During decompression biotite (Bt) is growing within the pressure shadows of the hinge areas of the crenulation cleavage (S2) (RSP53; Wölz Complex, Ramingstein Window; parallel Nicols).
- E) Paragonite-amphibolite showing the mineral assemblage ferro-tschermakite (Hb), paragonite (Pa), plagioclase (Pl), biotite, ilmenite (Ilm), magnetite and apatite. During decompression a symplectite of muscovite (Ms) and albite (Ab) developed along grain boundaries between amphibole and paragonite. (RSP45; Wölz Complex, Ramingstein Window; parallel Nicols).
- F) Polyphase garnet with a Permian core (Grt_p) and an Eoalpine rim (Grt_A) (RS44/97; Wölz Complex, Schöttel valley; parallel Nicols).
- G) Gneiss with polyphase garnets. The garnet core (Grt_H) is most probable Hercynian in age. Its outer part is rich in tiny inclusions. The garnet rim (Grt_A) grew during the Eoalpine metamorphic event (RSP20; Bundschuh Complex, Predlitz east of Ramingstein; parallel Nicols).
- H) Brittle deformed Eoalpine garnet crystals (Grt_A) within a mica-rich matrix. Aggregates of broken garnets give shear sense criteria for a top to northwest-directed deformation during the development of the mylonitic foliation (S1). Post deformed growth of the crystals caused a recovering of the crystal shape (RSP294; Wölz Complex, Ramingstein Window; parallel Nicols).

